microorganisms

MDPI

Article

Novel Insights on Extracellular Electron Transfer Networks in the *Desulfovibrionaceae* Family: Unveiling the Potential Significance of Horizontal Gene Transfer

Valentina Gonzalez [1,2,3], Josefina Abarca-Hurtado [1], Alejandra Arancibia [1,4], Fernanda Claverías [2], Miguel R. Guevara [5] and Roberto Orellana [1,4,6,*]

[1] Laboratorio de Biología Celular y Ecofisiología Microbiana, Facultad de Ciencias Naturales y Exactas, Universidad de Playa Ancha, Leopoldo Carvallo 270, Valparaíso 2360001, Chile; valentina.gonzalez.f10@gmail.com (V.G.); josefina.abarca@gmail.com (J.A.-H.); alejandra.arancibia@upla.cl (A.A.)
[2] Laboratorio de Microbiología Molecular y Biotecnología Ambiental, Departamento de Química & Centro de Biotecnología Daniel Alkalay-Lowitt, Universidad Técnica Federico Santa María, Avenida España 1680, Valparaíso 2390123, Chile; fclaveriasr@gmail.com
[3] Departamento de Química y Medio Ambiente, Sede Viña del Mar, Universidad Técnica Federico Santa María, Avenida Federico Santa María 6090, Viña del Mar 2520000, Chile
[4] HUB Ambiental UPLA, Universidad de Playa Ancha, Leopoldo Carvallo 207, Playa Ancha, Valparaíso 2340000, Chile
[5] Laboratorio de Data Science, Facultad de Ingeniería, Universidad de Playa Ancha, Leopoldo Carvallo 270, Valparaíso 2340000, Chile; miguel.guevara@upla.cl
[6] Núcleo Milenio BioGEM, Valparaíso 2390123, Chile
* Correspondence: roberto.orellana@upla.cl

check for updates

Citation: Gonzalez, V.; Abarca-Hurtado, J.; Arancibia, A.; Claverías, F.; Guevara, M.R.; Orellana, R. Novel Insights on Extracellular Electron Transfer Networks in the *Desulfovibrionaceae* Family: Unveiling the Potential Significance of Horizontal Gene Transfer. *Microorganisms* **2024**, *12*, 1796. https://doi.org/10.3390/microorganisms12091796

Academic Editor: Alejandro Rodriguez-Sanchez

Received: 22 June 2024
Revised: 24 July 2024
Accepted: 25 July 2024
Published: 29 August 2024

Copyright: © 2024 by the authors. Licensee MDPI, Basel, Switzerland. This article is an open access article distributed under the terms and conditions of the Creative Commons Attribution (CC BY) license (https://creativecommons.org/licenses/by/4.0/).

Abstract: Some sulfate-reducing bacteria (SRB), mainly belonging to the *Desulfovibrionaceae* family, have evolved the capability to conserve energy through microbial extracellular electron transfer (EET), suggesting that this process may be more widespread than previously believed. While previous evidence has shown that mobile genetic elements drive the plasticity and evolution of SRB and iron-reducing bacteria (FeRB), few have investigated the shared molecular mechanisms related to EET. To address this, we analyzed the prevalence and abundance of EET elements and how they contributed to their differentiation among 42 members of the *Desulfovibrionaceae* family and 23 and 59 members of *Geobacteraceae* and *Shewanellaceae*, respectively. Proteins involved in EET, such as the cytochromes PpcA and CymA, the outer membrane protein OmpJ, and the iron–sulfur cluster-binding CbcT, exhibited widespread distribution within *Desulfovibrionaceae*. Some of these showed modular diversification. Additional evidence revealed that horizontal gene transfer was involved in the acquiring and losing of critical genes, increasing the diversification and plasticity between the three families. The results suggest that specific EET genes were widely disseminated through horizontal transfer, where some changes reflected environmental adaptations. These findings enhance our comprehension of the evolution and distribution of proteins involved in EET processes, shedding light on their role in iron and sulfur biogeochemical cycling.

Keywords: sulfate-reducing bacteria; iron-reducing bacteria; extracellular electron transfer; mobilome

1. Introduction

Sulfate- and iron-reducing prokaryotes (SRPs and FeRPs) are microorganisms that play a vital role in the biogeochemical cycles of sulfur and iron, two essential elements for the functioning of life on earth [1,2]. A vast body of research highlights the impact of the interaction of these two groups across many ecosystems, including anaerobic soils and sediments, pristine or contaminated freshwater, groundwater and marine environments, and even intestinal systems [3–14]. The interactions between both functional groups

have been widely reviewed in marine environments, in which their activity accounts for most of the anaerobic organic matter degradation in sediments at the global level [15–19]. Currently, marine sulfate (~29 mM) is the largest mobile sulfur reservoir on our planet, an oxidizing pool even greater than atmospheric oxygen [20,21]. The mechanical and chemical weathering of continental rocks releases sulfur into the seawater column, which, in turn, continuously supplies sulfate to marine snow and sediments, where it is reduced by SRPs [16,20,22]. Analogously, iron enters the ocean from different sources, mainly remaining as a redox-active element in sediments, where FeRPs use it as an electron acceptor [3,23,24]. H_2, formate, acetate, and other volatile fatty acids produced by hydrolysis or fermentation are used as electron donors for both dissimilatory processes, making the biogeochemical cycling of carbon, iron, and sulfur tightly linked [10].

Major determining factors contribute to the balance of how iron and sulfate reduction are spatially and temporally organized [25]. First, there is a competition for electron donors that was initially addressed by studying the concept of competitive exclusion [11,26–30]. Second, these biogeochemical processes are constrained to those metabolisms that include dissimilatory pathways capable of interacting with insoluble (iron) and soluble (sulfate) electron acceptors and by the free energy released by each redox reaction. While dissimilatory iron-reducing metabolisms, which demand that electrons must be effectively transported from cytoplasmic donors to extracellular space and generate higher free energy, dominate surface environments where Fe (III) is available, reductions in sulfate, yielding less energy, are restricted to deeper layers of sediments [3,23,31]. Third, several chemical reactions regulate the bioavailability or toxicity of both substrates and by-products. For instance, Fe(II) produced by dissimilatory iron reduction tends to diffuse to an oxic/anoxic interface, where it is reoxidized back to Fe(III) [23,32]. In contrast, Fe(III) works as an oxidant for sulfide that is produced by deeper SRPs, producing iron sulfide (FeS) and, lately, pyrite [33], which competes with the incorporation of sulfide into organic matter [34–36].

Based on this evidence, it was initially assumed that iron and sulfate reductions occur in discrete zones [27,37,38]. However, more recent observations have challenged this notion, revealing that both processes can coexist simultaneously [3,13,14,39] and even interplay along different stages of mineral transformation [40]. Phylogenetically diverse species of SRPs can reduce Fe(III) and Mn(IV) as well as electrodes of bioelectrochemical systems, suggesting that these capabilities may be widespread in various clades, although few of them can conserve energy to support growth [23,41–48]. Several SRP strains have been involved in the corrosion of Fe-containing metals by a combination of different mechanisms, suggesting many possible pathways of interactions with extracellular electron donors/acceptors [49,50]. In addition, comparative genomic studies have shed light on the lasting role that genetic mobile elements play in the plasticity and evolution of genomes of members of the *Desulfovibrionaceae*, *Geobacteraceae*, and *Shewanellaceae* families [51–56]. Recent investigations have reported that genes encoding transmembrane electron conduits in *Shewanella*, MtrCAB and OmcA, have been disseminated through horizontal gene transfer within the same species [57], genus [58], and across distantly related genera [59], suggesting that the mobilome may play a role in acquiring sophisticated metabolic processes such as extracellular electron transfer (EET). This juxtaposition led to the hypothesis that as a result of co-localization, collaboration, and competition, as well as their metabolic plasticity, several SRPs may have also evolved the capability to reduce insoluble Fe(III) oxides coupled with the oxidation of low-concentration electron donors.

The *Geobacteraceae* and *Shewanellaceae* families are FeRPs that are well known for their EET capabilities. The mechanisms of their model bacteria, *G. sulfurreducens* PCA and *S. oneidensis* MR-1, have been extensively studied by combining genomic, transcriptomic, and proteomic approaches coupled with functional genetic experiments, and they have been expanded to other strains [60–65]. Based on these well-studied mechanisms, we conducted a search to understand the prevalence of the orthologs of EET-related proteins in forty-two genomes of SRB belonging to the *Desulfovibrionaceae* family. The analysis included 130 proteins that encode *c*-type cytochromes, such as porin–cytochrome complexes (Pcc),

b-type cytochrome complexes (Cbc), riboflavin biosynthesis genes, chemotaxis-related genes, and cell membrane components, and explored the mobilome of the three groups to assess the impact of horizontal gene transfer (HGT) on the acquisitions and losses of genes critical for EET by members of the *Desulfovibrionaceae* family.

Through phylogenetic and orthology analyses, we identified key proteins involved in EET that are widely distributed across these three families. Most of these proteins display modular diversification, serving as components of multiple complexes engaged in respiratory mechanisms. We believe this pool may include the essential core features required for the proper physiological functioning of EET and could constitute a crucial aspect of evaluating its expansion to other SRPs. These findings enhance our understanding of the evolution and distribution of proteins related to extracellular electron transfer processes, shedding light on their role in microbial communities actively participating in iron and sulfur biogeochemical cycles.

2. Materials and Methods

2.1. Genome Selection and Phylogenomic Analysis

A collection of already-sequenced genomes from both sulfate-reducing bacteria (SRB) and Fe-reducing bacteria (FeRB) were analyzed to investigate the shared genomic characteristics and the evolutionary relationships between the two groups. The selected genomes span 23 and 59 strains of the *Geobacteraceae* and *Shewanellaaceae* families, respectively, representing the FeRB, in addition to 42 genomes of SRB belonging to the *Desulfovibrionaceae* family (Table S1). The sequence data for all of the bacterial genomes were retrieved from the NCBI RefSeq database (query date: March 2022). The quality of the genomes was analyzed with CheckM [66], using completeness > 98% and contamination < 5% as the cutting parameters. In order to perform a genome-wide phylogenetic analysis between all selected genomes, OrthoFinder [67] was used to perform a DIAMOND-based all-versus-all gene search on amino acid levels and identify clusters of orthologous genes (OGs). From this analysis, 109 single-copy OGs were aligned by MAFFT [68] and concatenated to construct a phylogenomic tree with FastTree [69] under the maximum-likelihood method. For the visualization of the tree, MEGA X [70] and iTOL v5 [71] were used.

2.2. Creation of Custom Databases: Genes Related to Extracellular Electron Transfer (EET)

To identify EET-related genes in the selected genomes, a custom database was generated using 130 gene sequences reported to be involved in EET from two known FeRB: *Geobacter sulfurreducens* PCA and *Shewanella oneidensis* MR-1 (Table S2). This database includes several genes encoding *c*-type cytochromes, both outer-membrane and periplasmic; genes encoding porin–cytochrome complexes (Pcc) and *b*-type cytochrome complexes (Cbc); and genes related to riboflavin biosynthesis, chemotaxis, and cell membrane components, among others. The sequences were retrieved from the UniProt and NCBI NR databases (query date: January 2022).

2.3. Ecophysiological Analysis of SRB and FeRB

In order to relate and discover connections between the genomic and physiological characteristics of the bacteria analyzed, an extensive compilation of their ecophysiological information was carried out through a literature review, following and expanding what was previously described [53,72–198]. This analysis included the following parameters for each strain: (i) sources of isolation classified into the following categories: "Freshwater sediments", "Brackish water/sediments", "Marine water/sediments", "Soil", "Engineered/Impacted system", "Plant/Algae-associated", "Animal/Human-associated", "Food", and "Unknown"; (ii) growth conditions, such as pH and temperature growth ranges (with the terms "mesophile", "psychrophile", and "psychrotolerant" used as descriptors), and salinity tolerance, which was classified according to the maximum value of % NaCl in which growth was observed, or, if such information was not found, according to the source of isolation of each strain, classified as low (<1% NaCl, freshwater sediments/human-

associated), medium (1–3% NaCl, brackish water/sediments/marine animal-associated), or high (>3% NaCl, marine water/sediments); and (iii) metabolic traits such as oxygen tolerance (with the terms Anaerobe, Facultative anaerobe, or Aerobe), electron acceptors and donors used for growth (using the terms complete or incomplete oxidation), growth rate estimations based on duplication capacity under optimum conditions (as fast-growing: in ≤12 h, or slow-growing: in >12 h), and iron reduction capacity. This information was later connected to phylogenomic and similarity network analyses.

2.4. Comparative Genomics

To investigate the shared genomic features related to EET between the SRB and FeRB, a search was performed for the OGs inferred by Orthofinder containing sequences from our custom database. The presence or absence of proteins from each strain was evaluated by determining whether or not the genome possessed the correspondent OG. The inferred OGs containing the EET-related sequences of each genome were sorted according to the phylogenomic tree to generate a heatmap on the R platform with the gplots package v.3.0.3. The detected proteins were subsequently analyzed to predict their cellular localization using the PSORTb web server [199].

Multi-heme *c*-type cytochromes (≥3 CXX(X)H motifs) were identified with a Perl script [200]. The subcellular localization prediction for genes containing heme motifs was performed using PSORTb v3.0.3 [199]. The predicted categories were extracellular, outer membrane, periplasmic, cytoplasmic membrane, and unknown. In addition, a search for prophage-like sequences was carried out in all the analyzed genomes using the PHAge Search Tool Enhanced Release (PHASTER) web server (http://phaster.ca/ (accessed on 1 June 2022)) with default parameters for closed and WGS data [201]. Histograms with this information were performed using GraphPad Prism (version 8.2.1), and incorporated into the phylogenomic tree. The presence of CRISPR elements in the closed and WGS data of each strain was analyzed with the CRISPRCasFinder web server (https://crisprcas.i2bc.paris-saclay.fr/ accessed on July 2022) using the default parameters [202]. To quantify the number and type of insertion sequences (ISs) present in the genomes of each strain, the web server of ISFinder was used (https://isfinder.biotoul.fr/ (accessed on 30 July 2023)), using the default parameters for a blastn and an E-value of 0.000001 [203]. The ISs were considered if they had an alignment length over 700 bp. For the detection of integrons in the closed and WGS data of each strain, the program IntegronFinder was used in the open platform Galaxy@Pasteur (https://galaxy.pasteur.fr/ (accessed from July to September 2023)), using the default parameters with the addition of the option of local detection and a search of promoter and attI sites [204]. The 3 types of elements recognized by IntegronFinder were complete integrons (integrons with an integron–integrase near *attC* site(s)), In0 elements (integron–integrase only, without any *attC* site nearby), and CALIN elements (cluster of *attC* sites lacking a nearby integrase). To detect the number of types of ICEs present in each strain (including the ones in the chromosomes and plasmids sequences if they were available), the CONJScan models in MacSyFinder were used [205,206]. This was individualized by checking the number of proteins and the types of conjugation system for each strain.

2.5. Similarity Network

To search for evidence of the extracellular electron transfer potential in the groups of bacteria analyzed, a similarity network analysis was performed using the sequences of potential cytochromes (sequences containing greater than or equal to three heme motifs) predicted as the extracellular or outer membrane, according to the analysis using the PSORTb web server. For this purpose, all protein sequences from the OGs that contained at least one extracellular or outer-membrane cytochrome were extracted and used to perform a BLAST all-vs-all analysis. The network was generated with 1807 putative cytochrome sequences belonging to the *Desulfovibrionaceae* (125), *Geobacteraceae* (918), and *Shewanellaceae* (764) families. Each node in the network represents a single protein sequence and each

edge represents an alignment hit with an E-value of 10^{-40} or better. As filters for the network construction, an identity percentage of at least 30% and a minimum coverage of 70% were considered. The similarity networks were obtained using Gephi v.0.9.2 [207] with a combination of the Fruchtermann–Reingold [208] and Yifan Hu [209] layout algorithms. Community detection was performed using a weighted Louvain algorithm with a default resolution parameter of 1 [210].

2.6. Phylogenetic Analysis and Comparison of Genetic Contexts

The evolutionary relationship of the most prevalent EET-related genes shared between *Desulfovibrionaceae*, *Geobacteraceae*, and *Shewanellaceae* families was investigated using a phylogenetic analysis and the comparison of their genetic contexts. All the amino acid sequences of the OGs related to PpcA, OmpJ, CymA, CbcT, and CbcC were retrieved from the orthology analysis using Orthofinder. The gene trees of the selected OGs were recovered and visualized using iTOL v5 [71]. In addition, to facilitate the analysis of each OG, a sequence from each bacterium was chosen through local BLAST against the target protein, either from *Geobacter sulfurreducens* PCA or *Shewanella oneidensis* MR-1, and the visual comparison of their genetic contexts, giving greater priority to the latter. The selected amino acid sequences of each OG evaluated were aligned using MAFFT v7.511 [68]. The alignments were manually trimmed using the alignment editor AliView version 1.28 [211]. The phylogenetic reconstruction was determined by means of Bayesian Markov Chain Monte Carlo (MCMC) inference as implemented in MrBayes v3.2.7 [212]. Two independent runs were performed using a mixed amino acid substitution model where each run comprised 500,000 generations (two chains each run, sampling frequency of every 1000 generations). To construct the consensus tree, 25% of the trees were eliminated following a burn-in process. Posterior probabilities were used to support the internal branches. The visualization and editing of phylogenetic trees were performed using FigTree v. 1.4.4 software (http://tree.bio.ed.ac.uk/software/figtree/ accessed on 22 August 2024). Gene contexts were visualized using GeneSpy v1.2 [213], based on the GFF files from the NCBI RefSeq database.

2.7. Statistical Analysis

To understand how ecophysiological and genomic traits may influence the prevalence of elements related to microbial extracellular electron transfer (EET) in all the analyzed strains, we employed the statistical technique known as Principal Component Analysis (PCA). PCA is used for dimension reduction when dealing with numerous variables [214]. This analysis allowed us to use all the information provided by the various metrics without being biased by just a few aspects. Genomic traits (genome size and GC content), mobile genetic elements (number of prophages, CRISPR arrays, insertion sequences, integrons, and integrative and conjugative elements), and the number of copies of genes encoding proteins associated with EET-related elements (Cbc, CymA, Rib, OmpJ, and PpcA) were included in the analysis. Thus, PCA effectively splits genomes into groups reflecting both their sequence similarity and ecological distribution. PCA was performed using R software (version 4.3.1), selecting the first two principal components that captured most of the variance.

3. Results and Discussion

3.1. Phylogenomic Analysis of Sulfate-Reducing and Iron-Reducing Metabolism

To identify the shared genomic features between SRPs and FeRPs, a phylogenomic analysis including 124 genomes belonging to the *Desulfovibrionaceae*, *Geobacteraceae*, and *Shewanellaceae* families was reconstructed using 109 single-copy orthogroups (Figure 1). The analysis revealed that out of a total of 458,646 genes, 97.7% (448,320) were assigned to 15,156 orthologous groups (OGs). Of these, 289 OGs were present in all species, while 546 OGs were specific to certain species (Figure S1). The remaining unassigned genes and species-specific orthogroups represented the unique genetic traits of each species.

It was also found that the *Desulfovibrionaceae*, *Geobacteraceae*, and *Shewanellaceae* families share 2372 species-shared OGs and have 3300, 1737, and 4707 specific OGs, respectively. Interestingly, the *Desulfovibrionaceae* family shares a greater number of exclusive OGs with the *Shewanellaceae* family (1301) compared to the *Geobacteraceae* family (1088) (Figure S1).

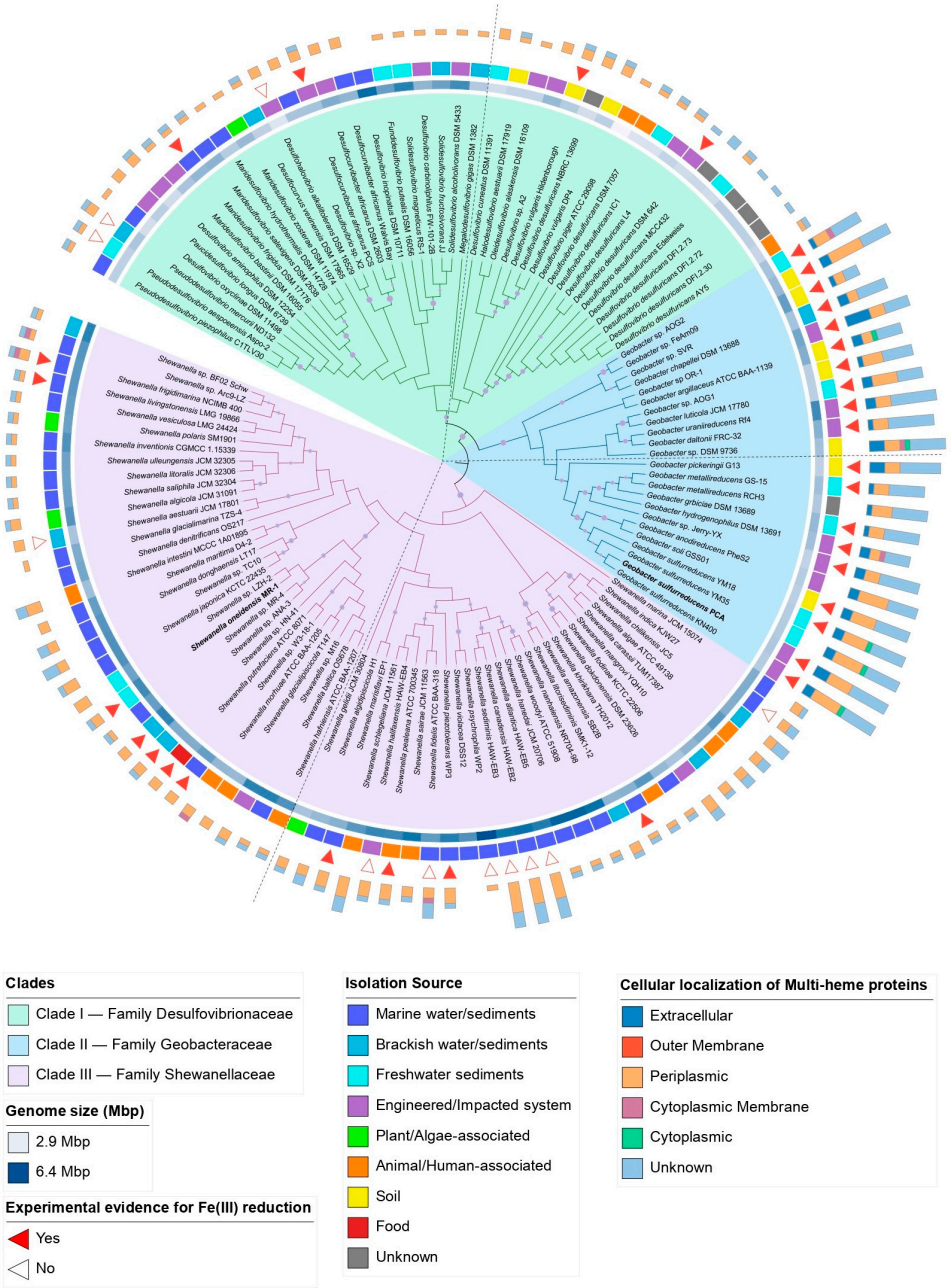

Figure 1. Phylogenomic cladogram of the analyzed genomes belonging to the *Desulfovibrionaceae*, *Geobacteraceae*, and *Shewanellaceae* families. Phylogeny was inferred using Orthofinder v2.5.4, identifying 109 single-copy orthogroups with all species present. Clades of each family are shown in colors. Blue scale rectangles beside the strains indicate a genome size from 2.9 to 6.4 Mbp. The adjacent squares represent the isolation sources. Red and white triangles indicate strains capable of/incapable of Fe(III) reduction in experimental assays. The absence of triangles indicates that no studies are available. The stacked bar graph shows the number of multi-heme *c*-type cytochromes (≥3 Cxx(x) H motifs) of each strain classified according to its cellular localization. *Geobacter sulfurreducens* PCA and *Shewanella oneidensis* MR-1 strains are shown in bold font. Bootstraps between 0.5 and 1 are indicated as purple circles of variable diameter in the respective node.

The resulting phylogenomic reconstruction revealed three major clades, each corresponding to each family. The *Desulfovibrionaceae* clade includes 42 genomes, most of which have been isolated or recovered from pristine and contaminated ecosystems, as well as from a broad range of aquatic environments, from marine sediments to freshwater (Tables S1 and S3 and Figure S2A). The *Desulfovibrionaceae* clade contains strains with an average genome size of 3.9 Mbp and a G+C content of 60.8%, with the smallest genome corresponding to *Desulfovibrio piger* ATCC 29098 (2.87 Mbp) and the largest to *Desulfovibrio inopinatus* DSM 10711 (5.77 Mbp). The *Desulfovibrionaceae* clade is divided into two distinct subclades. Subclade I mainly comprises strains living in marine and estuarine ecosystems, whereas subclade II comprises strains from freshwater and engineered ecosystems (Figure S2B). The *Geobacteraceae* clade includes 23 species of the *Geobacter* genus, a group of genomes belonging to species that have been isolated or recovered from soil and freshwater sediments as well as polluted sites, where *Geobacter* species play an important role in the regulation of biogeochemical cycles [215–219]. The *Geobacteraceae* clade contains strains with an average genome size of 4.0 Mbp and a G+C content of 58.3%. The smallest genome of this clade is *Geobacter benzoatilyticus* Jerry-YX (3.58 Mbp), and the largest genome is *Geobacter uraniireducens* Rf4 (5.14 Mbp). The *Geobacteraceae* clade is divided into two subclades. *Geobacter* strains isolated/found in soils, sediments, groundwater, and engineered environments belong to subclade I, while strains isolated from polluted sites and freshwater ecosystems belong to subclade II (Figure S2C). The third clade comprises 59 species of the *Shewanella* genus, with genomes with remarkably low values of G+C content (45.3%) and an average genome size of 4.8 Mbp. The *Shewanella* clade includes genomes ranging from 3.9 Mbp to 6.4 Mbp of *Shewanella aestuarii* JCM 17801 and *Shewanella psychrophila* WP2, respectively. Unlike the *Desulfovibrionaceae* and *Geobacteraceae* clades, 56% (33) of the species belonging to this clade have been isolated or recovered from marine ecosystems, and secondly, from samples derived from soils and sediments (subclade I) as well as freshwater and human- and animal-associated environments (subclade II), where *Shewanella* has been recently found (Figure S2D) [52,220].

As anticipated, our findings revealed variations in genomic traits, including GC content and genome size, among genomes from different subclades (Figure S3). In agreement with previous studies, the genomic GC content of strains of *Shewanellaceae*, a family within the class *Gammaproteobacteria*, was found to be lower than that of *Desulfovibrionaceae* and *Geobacteraceae*, which belong to *Deltaproteobacteria* [221]. Also, previous evidence has shown that genomes with higher GC content have more N in their proteomes [222]. Therefore, the lower GC content of *Shewanellaceae* strains may also be partially explained by the fact that several strains are primarily found in the ocean, an environment with a persistent limitation of N [223]. Another study reported that in the genome of *Desulfovibrio vulgaris*, mutations that convert GC to AT (GC->AT) were the most common, suggesting that a loss of GC content in this genome is slowly occurring [224].

In total, 34 strains out of the 124 surveyed had been implicated in some form of electron transfer to extracellular compounds, most of which belong to *Geobacteraceae* and *Shewanellaceae* clades. Both families have been the focus of a great extent of experimental evidence regarding their capabilities of extracellular electron transfer, which mainly relies on two types of mechanisms for electron transport across the outer surface. In *Shewanella* strains, substances that act as electron shuttles allow electrons to be transported from an intracellular enzymatic complex to the extracellular electron acceptor. This is the case with *Shewanella oneidensis* MR-1, which secretes small redox-active molecules for electron shuttling back and forth between cells and external electron acceptors [225]. In contrast, direct EET, which is prevalent in *Geobacter* strains, depends on the availability of redox-active enzymes and conductive appendages attached to the outer surfaces of the cells [226]. Four strains of the *Desulfovibrionaceae* clade, including *Maridesulfovibrio frigidus* DSM 17176 [46], *Desulfocurvibacter* africanus PCS [45], *Desulfovibrio vulgaris* str. Hildenborough [227], and *Desulfovibrio desulfuricans* DSM 642 [41], were shown to reduce Fe(III) and use it as an electron acceptor under experimental conditions. The extent to

which this process takes place under environmentally relevant conditions as well as their molecular mechanisms remain to be explored.

3.1.1. Abundance of Multi-Heme Cytochromes

Multi-heme *c*-type cytochromes (*c*-Cyts) are proteins that harbor three or more hemes that have a central coordinated Fe atom that allows for the transfer of electrons. In species like *Shewanella oneidensis* MR-1 and *Geobacter sulfurreducens* PCA, *c*-Cyts play a fundamental role in EET to solid metal (hydro)oxides [228–230] as well as direct interspecies electron transfer [231,232]. *c*-Cyts are also very abundant in *Desulfovibrionaceae* [233]. To assess the diversity and prevalence of *c*-Cyts, we searched for the motifs CXXCH and CXXXCH across all strains, revealing a total of 9800 such proteins. On average, members of *Geobacteraceae* have 125.7 heme-containing proteins per genome, whereas *Shewanellaceae* and *Desulfovibrionaceae* have 77.1 and 56.1, respectively. The CXXCH motif was more common than the CXXXCH motif, representing between 84.4% and 94.3% of all proteins with heme motifs (Figure 2A). Interestingly, some *c*-Cyts exhibited both motifs, though this was more prevalent in *Geobacter* proteins (9.6% of proteins exhibited both motifs) and rare in *Shewanella*. *Geobacter* strains had an average of 10.6 extracellular predicted *c*-Cyts per genome, compared to 1.1 *c*-Cyts per genome of the *Shewanellaceae* family, and none of the *Desulfovibrionaceae* (Figure 2B). Regarding the number of motifs found per protein, most contain only one or two motifs. This ranges between 52.5% in the *Geobacteraceae* family and 77.5% in the *Desulfovibrionaceae* family. The abundance of multi-heme cytochromes in *Geobacteraceae* strains is particularly interesting, with an average of 59.7 per genome, which is significantly higher than other families, which contain 12.6 and 24.6 multi-heme proteins per strain, respectively (Figures 1 and 2C). Some *Geobacter* strains, such as *G. uraniireducens* Rf4, *G.* sp. OR-1, *G. daltonii* FRC-32, and *G.* sp. DSM 9736, contain proteins with more than 40 heme motifs, whereas *Shewanella* and *Desulfovibrio* contain significantly less. In terms of cellular localization, it has been predicted that 9.5% of *Geobacter*'s multi-heme cytochromes and 0.7% of *Shewanella*'s are likely to be secreted from the cell. On the other hand, *Desulfovibrionaceae* strains do not seem to have extracellular multi-heme proteins or contain multi-heme proteins associated with the outer membrane (Figure 2). These findings agree with previous reports, where *Geobacter* species, such as *G. sulfurreducens*, encode many *c*-type cytochromes in their genomes compared to *Shewanella* and *Desulfovibrio* [64,233].

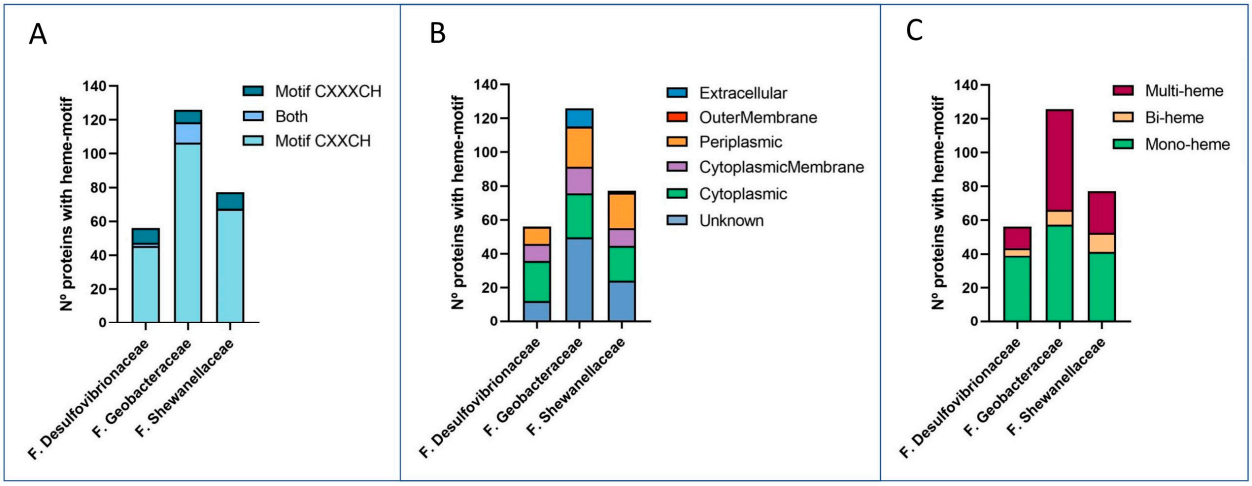

Figure 2. The abundance and diversity of proteins containing heme motifs in the *Desulfovibrionaceae*, *Geobacteraceae* and *Shewanellaceae* families. The average number of proteins containing heme motifs in the strains of each family, classified according to (**A**) type of heme motif, CXXCH, CXXXCH, or with both motifs; (**B**) cell localization predicted by the PSORTb web server, and (**C**) the number of motifs: mono-heme (1), bi-heme (2), and multi-heme (≥3).

3.1.2. Similarity Network Analysis of Extracellular Multi-Heme Cytochromes

A similarity network analysis was conducted to determine the phylogenetic relationships between the predicted multi-heme cytochromes located outside of cells. The analysis found 1807 sequences associated with 35 OGs (including some sequences that had not passed the extracellular localization filter). *Geobacter* strains had the majority of the sequences (918), followed by *Shewanella* strains (764) and *Desulfovibrionaceae* family strains (125). The similarity network had 130 sets of highly interconnected nodes (E-value threshold of 10^{-40}), known as communities, with 71 containing two or more nodes (Figure 3). The network clusters exhibited a clade-specific pattern, indicating closer relationships based on their family of origin. Despite no clear correlation between the isolation source and clusters, it is evident that cluster proteins related to *Shewanella* strains are adapted to high-salinity conditions due to their origin from marine sources (Figure S15). Some cytochromes involved in EET, including OmcA and MtrC from *S. oneidensis* MR-1, and OmcA, OmcS, OmcZ, and CbcA from *G. sulfurreducens* PCA, are exclusively grouped with cytochromes of the same family. However, the OmcI cytochrome of *G. sulfurreducens* PCA, and the DsmE and MtrA cytochromes of *S. oneidensis* MR-1, were grouped in the same cluster along with other cytochromes of the *Shewanellaceae* and *Geobacteraceae* families. On the other hand, the *Desulfovibrionaceae* family presents nodes related to six clusters, three of which contain at least two cytochromes belonging to *Desulfovibrionaceae* strains capable of Fe reduction. The first of these clusters (community N#37, Figure 3B) is comprised exclusively of proteins of this family, whose products correspond to cytochrome *c* family proteins containing ten heme motifs. The second cluster (Figure 3C) contains 65 sequences (community N#33) encoding for a cytoplasmic membrane-bound cytochrome ubiquinol oxidase subunit I or *c*-type cytochromes. Both clusters related to OG 517 and OG 1638 also contain some *Geobacter* and *Shewanella* cytochromes predicted to be extracellular, and therefore, exploring their function in future studies may be interesting.

3.1.3. Comparative Genomic Analysis of Genes Related to Extracellular Electron Transfer Mechanisms

Since several molecular mechanisms for which members of the *Geobacteraceae* and *Shewanellaceae* families interact with extracellular electron acceptors have been widely described, we analyzed the dataset of *Desulfovibrio* genomes to learn about the ubiquity and abundance of proteins involved in EET (Figure 4). To conduct the analysis, we identified EET-related proteins in each genome by checking for their presence in the corresponding orthologous groups (OGs) from *S. oneidensis* MR-1 or *G. sulfurreducens* PCA. We evaluated 130 genes that encoded both outer-membrane and periplasmic *c*-type cytochromes, genes encoding porin–cytochrome complexes (Pcc) and *b*-type cytochrome complexes (Cbc), riboflavin biosynthesis genes, genes related to chemotaxis, and cell membrane components (Table S2).

Similarities with the EET Mechanism of *G. sulfurreducens*

Investigations focused on *Geobacter* models, such as *G.sulfurreducens* and *G. metallireducens*, contributed to the comprehension of EET through multiple respiratory pathways [64,215,234]. These mechanisms mainly involve *c*- and *b*-type cytochromes in the inner membrane, ImcH and CbcL. The deletion of these genes impaired the ability to reduce electron acceptors with potentials above and below −0.1 V versus the standard hydrogen electrode (SHE) [235,236]. While both proteins have orthologs in all tested *Geobacter* species, only four *Desulfovibrionaceae* strains have CbcL homologs, including *M. frigidus* DSM 17176, a strain capable of Fe(III) reduction, but incapable of producing enough energy to support growth [46] (Figure 4). The genome of *G. sulfurreducens* contains four gene clusters encoding inner-membrane cytochromes, including Cbc3 (*cbcVWX*), Cbc4 (*cbcSTU*), Cbc5 (*cbcEDCBA*, where *cbcC* is also known as *omcQ*), and Cbc6 (*cbcMNOPQR*), that play a role in EET [64]. The deletions of *cbcV* and *cbcBA* resulted in a considerable decrease in Fe(III) reduction, and a transcriptional study found that cbcT was upregulated on insoluble metal

oxides versus Fe(III) citrate [64,237,238]. All these gene clusters are conserved and widely distributed in all *Geobacter* species [239], except for the Cbc6 cluster, which is incomplete in seven strains, mainly belonging to *Geobacter* subclade I (Figure 5). The CbcOP subunits are CbcVW orthologous proteins from the Cbc3 cluster and are present in all *Geobacter* and *Shewanella* strains but only in a few strains of the *Desulfovibrionaceae* family.

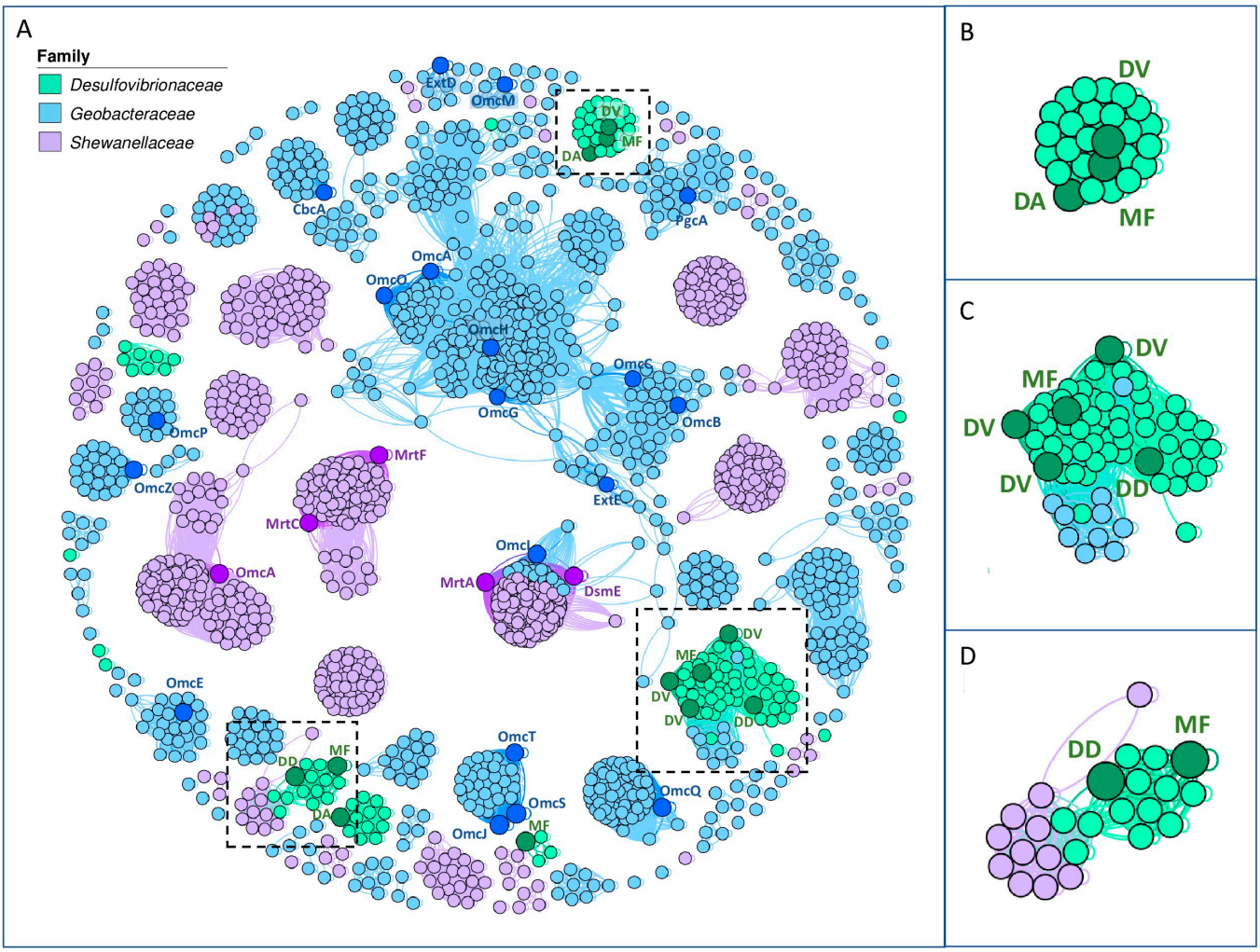

Figure 3. Multi-heme cytochrome similarity network. The distance network was constructed based on the protein sequences present in OGs containing multi-heme cytochromes (1807 sequences) predicted as extracellular from the 124 genomes of *Desulfovibrionaceae* (125 sequences), *Geobacteraceae* (918 sequences), and *Shewanellaceae* (764 sequences) families. The E-value threshold of the blast alignment for the network is 10^{-40}. Each node represents an extracellular multi-heme cytochrome, and the color fill indicates the origin of the sequence. The family *Desulfovibrionaceae* is green, the family *Geobacteraceae* is blue, and the family *Shewanellaceae* is violet. The nodes highlighted in a larger and more intense color show previously studied cytochromes of known metal-reducing bacteria, in blue for *G. sulfurreducens* PCA and violet for *S. oneidensis* MR-1. Green highlights the cytochromes of the bacteria *Desulfocurvibacter* africanus PCS, *Desulfovibrio desulfuricans* DSM 642, *Desulfovibrio vulgaris* str. Hildenborough, and *Maridesulfovibrio frigidus* DSM 17176, which have also been reported to show Fe(III) reduction. These cytochromes are highlighted by their initial letters, DA, DD, DV, and MF. (**A**) Entire network. (**B**–**D**) Zooming into particular network clusters possessing at least two cytochromes of the metal-reducing bacteria of the *Desulfovibrionaceae* family mentioned above.

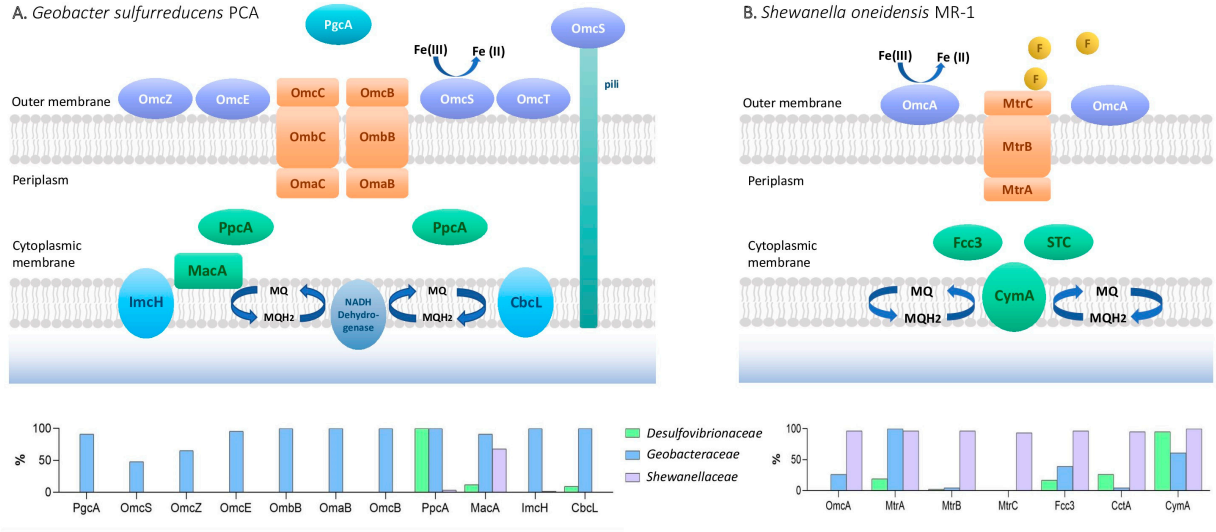

Figure 4. Proposed mechanisms for bacterial EET in model FeRB. The figures represent the mechanisms of *Geobacter sulfurreducens* PCA and *Shewanella oneidensis* MR-1. At the bottom, the bar plots show the percentage of the genomes in a given family that encode each EET-related gene.

Among the periplasmic cytochromes, PpcA, MacA, and PccF have been characterized in more detail. It has been proposed that PpcA transfers electrons from the cytoplasmic membrane to the outer membrane, while MacA acts as a hydrogen peroxide reductase and transfers electrons to PpcA [240,241]. The expression of the gene encoding PccF was upregulated during growth on insoluble metal oxides, suggesting a possible role during EET [237]. Homologs of these three genes were heterogeneously distributed across the members of the three families. While several genes encoding PpcA were highly abundant in *Geobacter* (average of 4.9 genes per genome) and *Desulfovibrio* (average of 3 genes per genome), the gene encoding MacA was mostly shared between *Shewanella* and *Geobacter* strains (Table S2). A porin–cytochrome complex (Pcc) capable of transferring electrons across a liposomal membrane is encoded by a periplasmic *c*-type cytochrome (OmaB/C), a porin-like protein (OmbB/C), and a reductase (OmcB/C). The Pcc protein complex reduces ferric citrate and ferrihydrite, similar to the MtrABC complex in *S. oneidensis* [242]. Three additional gene clusters encoding putative "electron conduits" involved in EET, including the porin–cytochrome (Pcc) complex extABCD, the porin–cytochrome (Pcc) complex extEFG, and the porin–cytochrome (Pcc) complex extHIJKL [243], were found to be highly prevalent in *Geobacter* species. However, no homologs were found in the *Shewanellaceae* and *Desulfovibrionaceae* family members (Figure 5). A similar distribution was found in the plethora of multi-heme *c*-Cyts associated with the outer membrane, including OmcS, OmcZ, OmcE, OmcT, and PgcA, which play different roles along the EET for both Fe (III) and Mn(IV) oxide reduction and electrode respiration (Figures 5 and S4) [237,244–249]. In contrast, genes encoding the outer-membrane *c*-Cyts OmcI, a homolog of the CbcA subunit of *G. sulfurreducens*, and the outer-membrane protein J (ompJ), a channel known to influence the quantity and localization of cytochromes in the outer membrane [250], were found to be present in all the strains of *Geobacteraceae* and *Desulfovibrionaceae*, and partially in *Shewanellaceae* strains. Xap, an extracellular anchoring polysaccharide protein, has a crucial role in metal oxide attachment, cell–cell agglutination, and localization of essential *c*-Cyts. It possesses averages of 35, 29, and 23, high numbers of homologs, in the *Desulfovibrionaceae*, *Geobacteraceae*, and *Shewanellaceae* families, respectively [251]. Although recent evidence has highlighted the role of secreted riboflavins during DIET in *Geobacter* cocultures [252], this mechanism was not added to our analysis.

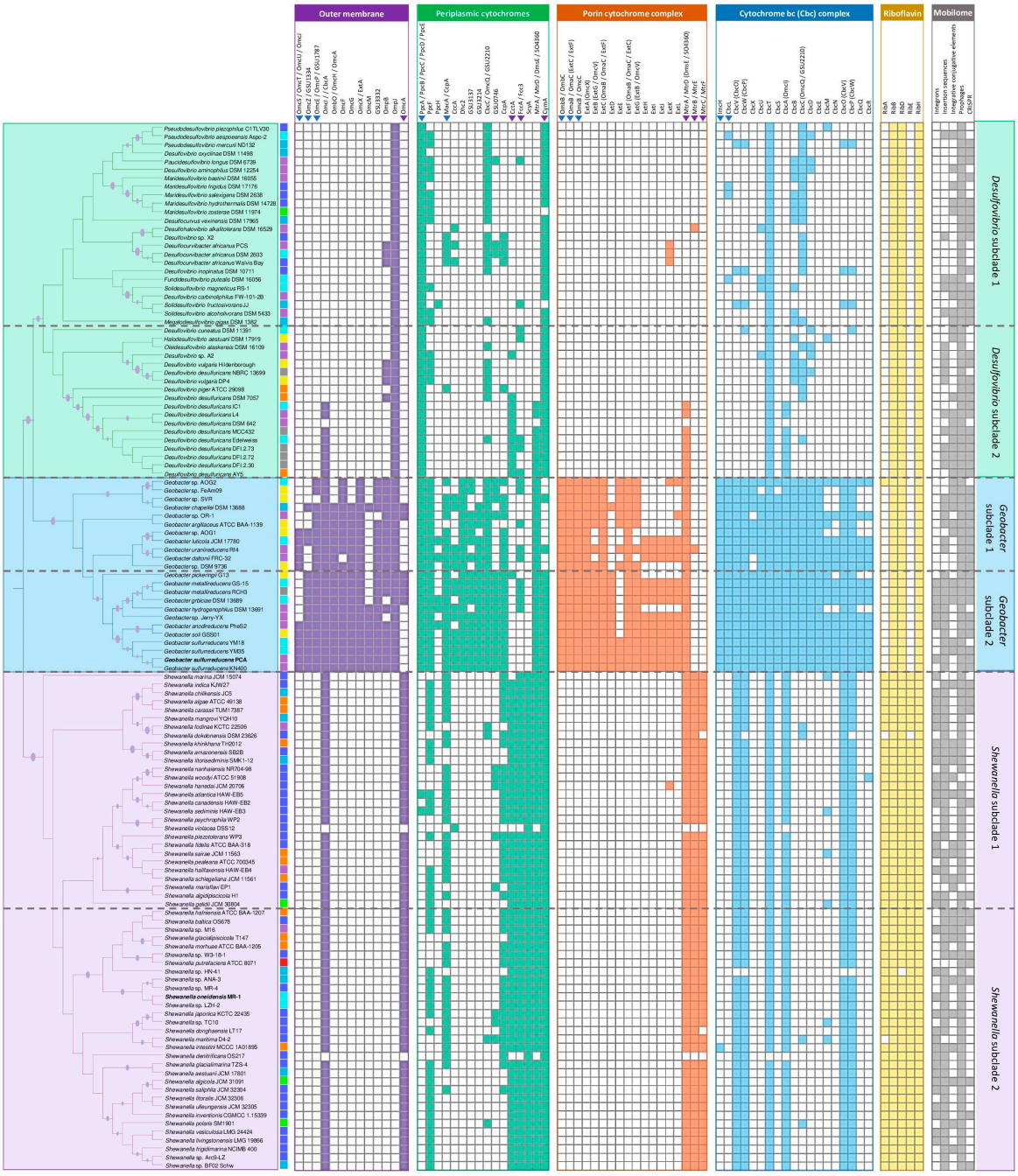

Figure 5. The presence/absence matrix of genes in OGs related to the EET mechanisms of *S. oneidensis* MR-1 y *G. sulfurreducens* PCA. On the left, the phylogenomic cladogram is presented with the isolation source. Boxes indicating the presence or absence of genes in the OGs involved in EET mechanisms are colored according to cell localization as follows: purple for outer-membrane cytochromes/proteins, green for cytochromes and proteins located in the periplasm, orange for porin–cytochrome complexes, blue for cytochrome bc (Cbc) complexes, and yellow for genes involved in riboflavin biosynthesis. The blue and purple triangles on the heatmap report the relevant genes in the EET mechanisms of *G. sulfurreducens* PCA and *S. oneidensis* MR-1, respectively.

Similarities with the EET Mechanism of *Shewanella oneidensis*

EET is mediated by CymA, a six multi-heme *c*-Cyts, in *S. oneidensis* MR-1. CymA oxidizes quinol in the cytoplasmic membrane and transfers electrons to Fcc3 and STC, which transport electrons to MtrA [253–255]. MtrA, MtrB, and MtrC form a trans-outer-membrane

complex to transfer electrons to the bacterial surface. MtrC and OmcA can physically interact with each other and transfer electrons directly to Fe(III) minerals [256–258], as well as associate with extracellular structures that were previously referred to as 'nanowires' [259]. *S. oneidensis* MR-1 employs endogenously produced flavin electron shuttles to enhance EET to minerals and electrodes during anaerobic respiration. Thus, released flavins are proposed to function as diffusive electron shuttles that transport electrons from MtrC and OmcA to mineral surfaces [225,260,261]. Homologs of CymA were found ubiquitously in all three families analyzed, with the exception of genomes of strains belonging to *Geobacter* subcluster I. In contrast, homologs of OmcA were found to be distributed in almost all the species of *Shewanella* and a few of *Geobacter* (Figure 5). Whereas Fcc3 homologs were found mainly in *Shewanella* strains, homologs of cctA, the gene coding the tetraheme STC, were shared by *Shewanella* strains and all strains of *Desulfovibrio desulfuricans* (Figures 5 and S4). In addition to that, one guanosine triphosphate (GTP) and two ribulose-5-phosphate molecules are converted into one riboflavin molecule in a stepwise manner by the enzymes encoded by the ribA, ribB, ribD, ribH, and ribE genes [262]. This pathway seems to be ubiquitous in *Shewanella* species, although homologs of some of these genes, specifically ribB, ribD, and ribH, are also found in all species belonging to the *Geobacteraceae* and *Desulfovibrionaceae* families, which could imply some role of these molecules in their EET mechanisms. Further experimental research is required to investigate if flavins play a relevant role during EET by SRPs, as the addition of riboflavin and flavin adenine dinucleotide (FAD) showed the accelerated corrosion of carbon steel and stainless steel by *D. vulgaris* [263,264].

3.2. Mobilome Analyses across Members of Desulfovibrionaceae, Geobacteraceae, and Shewanellaceae Families

The genetic makeup of prokaryotic genomes is composed of DNA fragments from both vertical and horizontal gene transmission. The mobilome, a collection of mobile genetic elements, facilitates the transfer of genes and their corresponding functions within a community through horizontal gene transfer (HGT) [265]. Our analysis reveals that these SRP and FeRP families host various mobile genetic elements, such as plasmids, bacteriophages, integrons, insertion sequences (ISs), and integrative and conjugative elements (ICEs). According to a PHASTER search, 333 prophages were found in total, with 59 intact, 244 incomplete, and 30 questionable phages present in 122 strains (Figure 6A). The average number of prophages per strain was 3.1, 2.7, and 2.5 in *Desulfovibrionaceae*, *Geobacteraceae*, and *Shewanellaceae*, respectively. This variation is influenced by a combination of genomic, phenotypic, and environmental factors, including genome size, physiological status, and the specific habitat in which the strain resides [266–268]. Our findings revealed that strains from *Desulfovibrio* subclade II and *Geobacter* subclade I, predominantly present in soils, freshwater, subsurface, and engineered ecosystems, exhibited the highest prophage density (prophages per Mbp genome). In contrast, strains from *Shewanella* subclade I and *Desulfovibrio* subclade I, more prevalent in marine environments, displayed the lowest values (Figure S5). Clustered regularly interspaced short palindromic repeats (CRISPR) is a system that allows the identification and cleavage of foreign DNA. The presence of CRISPR-Cas arrays constitutes a barrier to HGT, including natural transformation, transduction and conjugation [269–271]. Our analysis revealed a high prevalence of CRISPR arrays in the genomes of *Desulfovibrionaceae* and *Geobacteraceae*, while a significantly lower prevalence (less than 30%) was observed for *Shewanellaceae* strains (Figure 6B). This trend could be explained by the recent identification of phages with genes encoding proteins capable of inhibiting CRISPR-Cas function in several *Shewanella* strains [272–274]. Integrons are genetic units that capture genetic material in bacteria, adding novel features to the cell that contains it. They consist of an integron–integrase gene, an integration site, a promoter for gene cassettes, and up to 200 gene cassettes containing open reading frames flanked by *attC* recombination sites [275,276]. We found complete integrons in over 50% of strains of *Shewanellaceae* and subclade II of *Geobacteraceae*, while they were absent in the other clades. A similar pattern was found for the prevalence of insertion sequences (ISs), which are cryp-

tic DNA segments containing passenger genes that contribute to the metabolic plasticity and evolution of microbial genomes [277,278]. Our results indicate that the prevalence and number of ISs are unevenly distributed across the different bacterial groups included in this study. The *Shewanella* and *Geobacter* genomes contained 584 (~10.8 IS per genome) and 234 (~13 IS per genome), respectively, while the *Desulfovibrio* genomes contained a total of 34 ISs (~2.3 ISs per genome), with 27 out of the 42 *Desulfovibrio* showing no detection of ISs (Tables S4 and S5). With few exceptions, including *Desulfovibrio vulgaris* str. Hildenborough, the low prevalence of ISs in *Desulfovibrio* species is consistent with previous studies, suggesting limited genomic rearrangements by transposition in this genus [279,280]. This may be explained by the fact that some of the ISs found to belong to families (i.e., IS*Dvu3*) in which the control of transposase expression relies on stop codon read-through and, therefore, may be affected by other regulatory mechanisms [281]. Between 35 and 61% of genomes were found to contain integrative and conjugative elements (ICEs). In agreement with previous reports and in contrast to what was found with integrons and ISs, strains belonging to Shewanellaceae registered a lower prevalence of ICEs than the other two families [52].

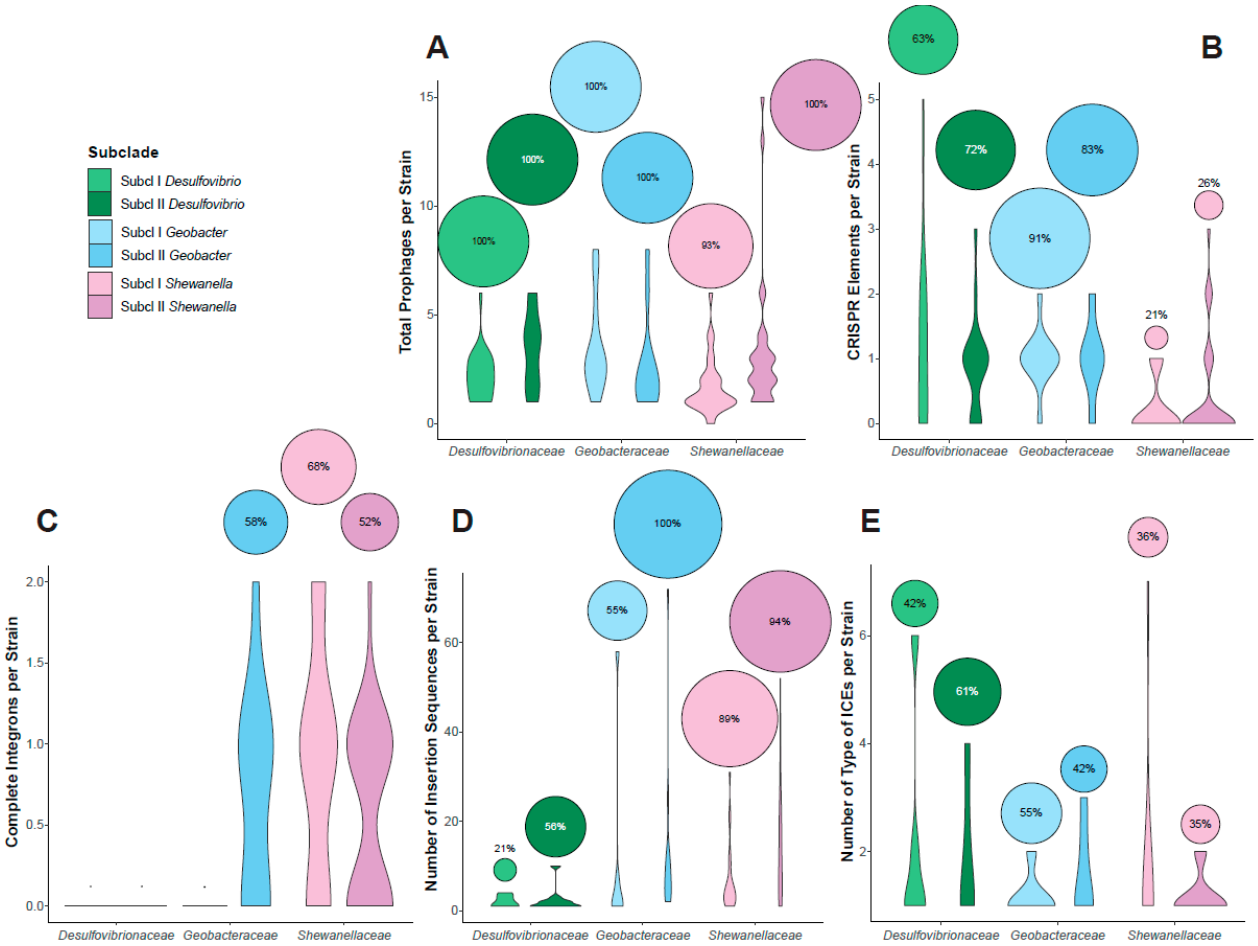

Figure 6. Violin plots representing the distribution of elements associated with the mobilome across different subclades and families; (**A**) total prophages per strain, (**B**) CRISPR elements per strain, (**C**) complete integrons per strain, (**D**) number of insertion sequences per strain, and (**E**) number of types of ICEs per strain. The circles on the top represent the prevalence of each element found in each family. Dots on the top represent that no strain was found to contain integrons.

The data from 124 genomes were used to conduct a Principal Component Analysis (PCA) of thirteen genomic and mobilome variables and metrics reflecting the prevalence of EET elements (Figure 7). The analysis clustered the strains into three big groups on the

PC1-PC2 plane (accounting for 50.88% of the total data variability), revealing a stronger correlation with the taxonomy of species than with their habitats (Figure S6). Based on the number of copies of genes encoding CymA, PpcA, and riboflavins, the number of CRISPR arrays and integrons per genome, genome size, and GC content, the *Shewanellacea* group is farther from the *Geobacteraccea* and *Desulfovibrionaceae* groups. The latest two groups are separated along the PC2, which includes the number of total cytochromes and genes encoding OmpJ and Cbc-related genes, as well as PpcA, which is almost absent in *Shewanellaceae* strains (Figures 5, S4 and S6). Interestingly, the number of copies of genes encoding proteins related to EET contributes to the differentiation within the three groups. While the number of copies of genes encoding for CymA and riboflavins contributed to the distinction between *Shewanella*, the number of copies of genes encoding for OmpJ contributed to the distinction of the *Desulfovibrionaceae*. In a similar manner, the number of copies of genes encoding for Cbc and total cytochromes contributed to the distinction of the *Geobacteraceae* and the other two groups. Thus, this result suggests that the prevalence and abundance of EET elements significantly contributed to the differentiation of these groups.

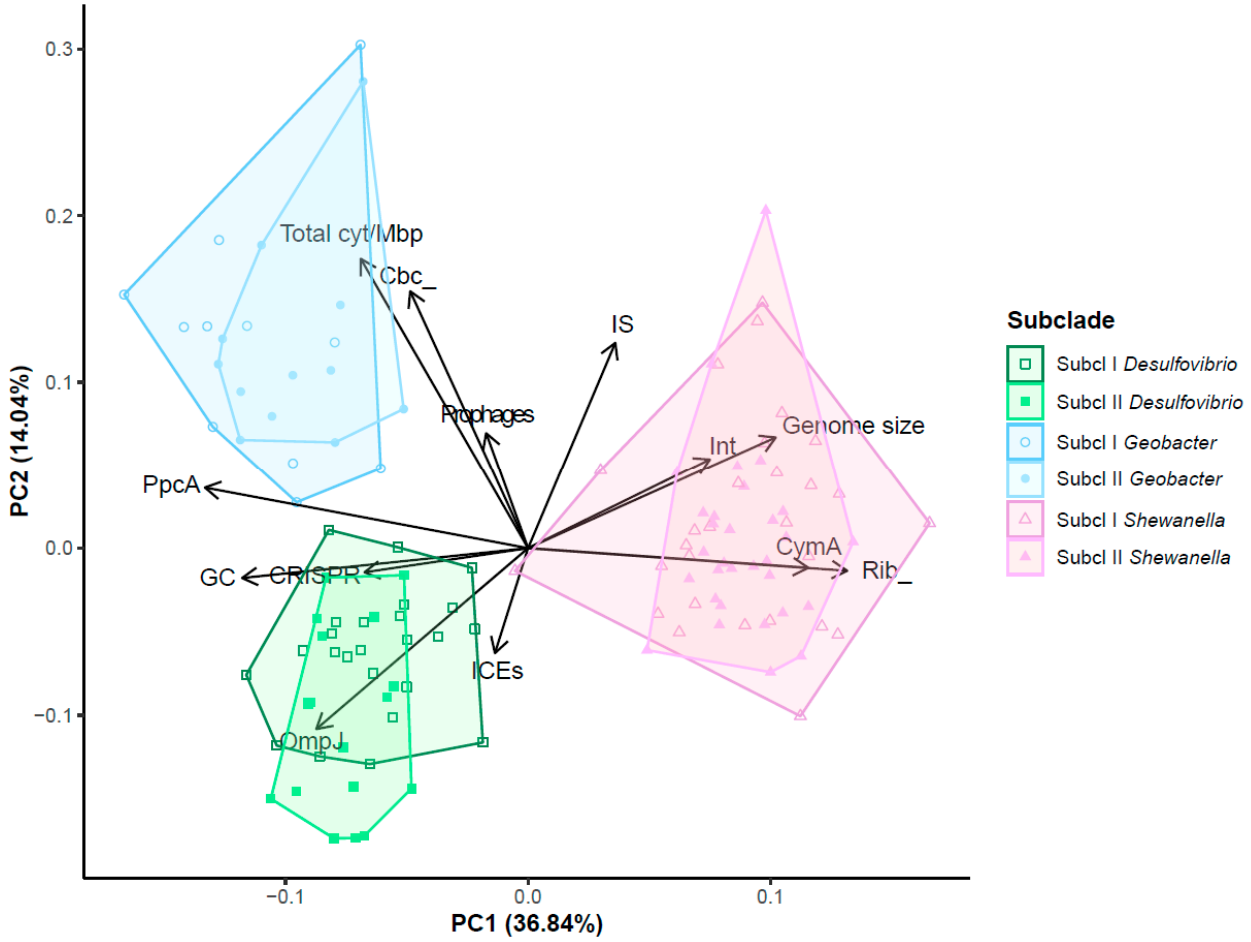

Figure 7. Principal Component Analysis of the strains from the *Desulfovibrionaceae*, *Geobacteraceae*, and *Shewanellaceae* families in relation to their mobilome components, types of cytochromes, genome size, and GC content. The strains were compared with the following parameters: genome size (Genome_size), GC% (GC), total prophages per strain (Prophages), total cytochromes per Mbp (Total cyt/Mbp), complete integrons per genome (Int), CRISPRs (CRISPR), number of insertion sequences per strain (IS), types of ICEs per strain (ICEs), number of copies of PpcA per strain (PpcA), number of copies of OmpJ per strain (OmpJ), sum of the number of copies of Cbc (Cbc_), number of copies of CymA (CymA), and sum of the number of copies of Rib (Rib_). The shapes indicate which family the strain is from, and the filling/color indicates the corresponding subcluster.

3.3. Evolutionary Relationship of the Most Prevalent EET-Related Genes in SRPs

Many of the genomes belonging to the *Desulfovibrionaceae* family were found to possess genes homologous to crucial proteins involved in the EET mechanisms of *S. oneidensis* MR-1 and *G. sulfurreducens.* This includes the triheme periplasmic cytochrome PpcA, the outer-membrane protein OmpJ, the tetraheme *c*-type cytochrome CymA, the iron–sulfur cluster-binding protein CbcT (a subunit of the Cbc4 complex), and, to a lesser extent, the cytochrome *c*-type CbcC (a subunit of the putative Cbc5 complex). All of these exhibited widespread distribution within this family. To gain insights into the evolutionary relationship of these shared genes among the *Desulfovibrionaceae*, *Geobacteraceae*, and *Shewanellaceae* families, we conducted phylogenetic analysis and compared the genetic contexts of the select genes associated with the orthologous groups of these candidate proteins.

3.3.1. The Periplasmic Cytochrome PpcA, an Intermediary in Extracellular Electron Transfer

PpcA is a periplasmic cytochrome that acts as an intermediary electron carrier for EET. Genetic studies have found that PpcA acts as a terminal reductase for anthraquinone-2,6-disulfonate (AQDS), Fe(III)-citrate, and Ferric nitrilotriacetate (Fe-NTA), although this gene was not differentially expressed when *G. sulfurreducens* was grown with Fe(III) citrate and Fe(III) oxide [240,282,283]. The genetic context of *ppcA* in *G. sulfurreducens* includes several adjacent genes encoding *c*-type cytochromes, as well as genes involved in their biogenesis, such as ResB and CcsB [284], and genes involved in the biosynthesis of menaquinones and ubiquinones, redox-active compounds involved in respiratory networks [285,286] (Figure S7). The genomic context remains largely invariant across different species, and its phylogenetic relationship aligns with the species' phylogenomic tree, suggesting vertical transmission rather than horizontal gene transfer.

PpcA is part of a family of five periplasmic triheme cytochromes (including PpcB, PpcC, PpcD, and PpcE). Thermodynamic characterization of those cytochromes revealed differences in their heme reduction potentials, allowing for a wider range of redox partners and enhancing the adaptability of the respiratory mechanism [287,288]. Our findings revealed that ppcA homologs are prevalent in *Geobacter* species, with most strains containing between 5 and 6 homologous genes, averaging 4.9 genes per strain. Notably, ppcA homologs were also present in all examined members of the *Desulfovibrionaceae* family, with the majority of those having between 3 and 4 homologous genes (averaging about 3.4 genes per strain) (Tables S2 and S6).

The phylogenomic analysis identified four primary clades within the PpcA protein family (Figure 8). Clade 1 exclusively consists of proteins from *Geobacter* strains. Notably, the five known homologous proteins from *G. sulfurreducens* (PpcA, PpcB, PpcC, PpcD, and PpcE) are distributed across different subclades within this group. Proteins similar to PpcA from the *Desulfovibrionaceae* family, found in the remaining three clades, exhibit significant diversification within their respective subclades. Similar to *Geobacter*, the presence of multiple variants and their diversification is likely the result of functional diversification associated with heme reduction. One example of evolutionary divergence is the gene encoding for the PpcA protein of *Pseudodesulfovibrio mercurii* (WP_014320801.1), which, based on genomic context, falls outside the four main clades (Figures S7 and S8). The unique environmental characteristics of the mid-Chesapeake Bay estuarine sediments where *P.mercurii* was isolated, including complex geochemical processes, nutrient-rich reducing waters, and the presence of rare earth elements (REEs), such as Cerium (Ce) and Europium (Eu), might have been significant factors driving this divergence [289,290]. In contrast, homologs of *ppcA* in two *Shewanella* strains, *S. atlantica* HAW-EB5 and *S. sediminis* HAW-EB3, both isolated from marine sediments near Halifax Harbour, Canada [291,292] suggest a horizontal gene transfer (HGT) event from another bacterium in this geographical region. Furthermore, clade 2 mainly comprises homologous proteins from members of the *Desulfovibrionaceae*, except for a PpcA homologous from *Geobacter* sp. SVR (WP_239077329.1), suggesting potential horizontal gene transfer events based on an interruption in the phylogenetic tree

topology. These assumptions are supported by the presence of transposase-encoding genes in the vicinity of these genes [293,294].

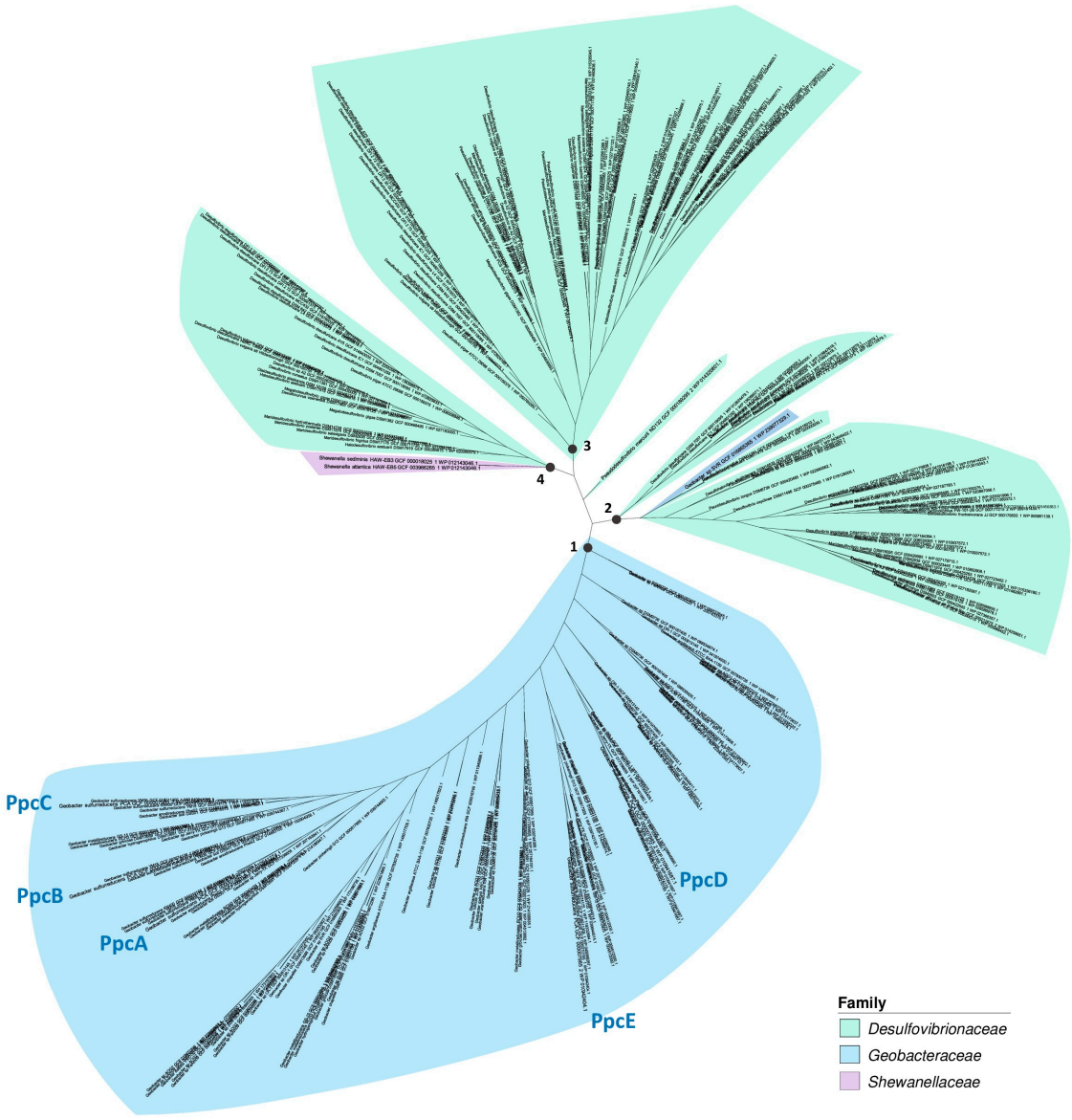

Figure 8. Phylogenetic tree of proteins homologous to PpcA. The phylogenetic tree was inferred using Orthofinder v2.5.4, and corresponds to the orthologous group where the periplasmic triheme cytochrome PpcA is present. The tree is composed of 257 protein sequences: 112 from *Geobacter* strains, 2 from *Shewanella*, and 143 from members of the *Desulfovibrionaceae* family. Each clade/branch is colored according to its family of origin. In the figure, the positions of PpcA and its homologs PpcB, PpcC, PpcD, and PpcE in *G. sulfurreducens* PCA are indicated.

3.3.2. OmpJ, an Integral and Widespread Outer Membrane Protein in the Desulfovibrionaceae Family

Homologs of OmpJ were found to be widely distributed in the *Desulfovibrionaceae* family. Similar to *Geobacter* species, most of these strains have between one and two homologous ompJ genes. Interestingly, *Desulfovibrio desulfuricans* strains and those from the *Solidesulfovibrio* genus stand out, with most of their members having between eight and ten genes homologous to ompJ (Tables S2 and S6). This substantial prevalence of OmpJ-like genes suggests that this protein may have a role in the physiology, adaptation, and capabilities of participating in sulfate reduction and metallo-reduction processes [41].

The distribution of the ompJ phylogenetic tree shows three clear groups: one from *Geobacter* and two from the *Desulfovibrionaceae* family (Figure S9A). The two branches of the *Desulfovibrionaceae* family consist mainly of species isolated from marine environments, pollution events, or industrial activity, while the other group primarily comprises species isolated from soil, freshwater, or animal sources (Figure S10). One exception is *Halodesulfovibrio aestuarii* DSM 17919, isolated from shoal mud in Germany [295], which stands out as it harbors two similar proteins that are significantly different from the other genes. This discrepancy in the species tree may suggest a horizontal transmission event, since near these ompJ-homologous genes, several tRNA sequences are found. To date, there have been limited reports regarding the function of OmpJ. Therefore, it would be of interest to assess its potential role in signaling mechanisms and its impact on EET mechanisms.

3.3.3. CymA, a Common Branch Point in the Electron Transport Chain

The *c*-type cytochrome CymA seems to be essential for facilitating the anaerobic respiratory adaptability of *Shewanella*. CymA plays a key role in transferring electrons from menaquinol to various systems responsible for reducing terminal electron acceptors, such as fumarate, nitrate, nitrite, dimethyl sulfoxide (DMSO), arsenate, and insoluble minerals like Fe(III) and Mn(IV) [253,296–298]. Homologous genes to cymA are widespread among the members of the analyzed families. The phylogenetic tree of CymA reveals three main clades: two from *Shewanella* strains and a third shared between strains of *Geobacter* and the *Desulfovibrionaceae* family. While *Shewanella* species contain between 1 and 5 homologs (with an average of 2.7), almost all members of the *Desulfovibrionaceae* family contain 1 or 2 homologs, with a few exceptions. Nearly half of the species analyzed in *Geobacteraceae* contain one to two genes homologous to cymA (Tables S2 and S6). The variable presence of these genes in *Geobacteraceae* species suggests two potential evolutionary scenarios: the genes were either lost in most species or inserted into the genomes of the analyzed species. Notably, species containing these genes are mostly clustered within a specific clade in the phylogenetic tree (Figures S11 and S12), hinting at the likely insertion of this gene through horizontal gene transfer into the common ancestor of these species, followed by its subsequent vertical transmission. Another notable sequence in the phylogenetic tree is one of the homologous copies from *Geobacter hydrogenophilus* DSM 13691 (WP_214187890.1), positioned between two subclades of *Desulfovibrionaceae* family proteins (Figure S9B). The context of this sequence suggests it was likely acquired via horizontal gene transfer, especially considering the proximity of genes encoding site-specific integrases and recombinase family proteins. Interestingly, when investigating the gene contexts of cymA homologs, several members of the *Desulfovibrionaceae* and *Geobacteraceae* families feature one of these homologous genes located near the gene encoding ammonia-forming cytochrome c nitrite reductase subunit c552 (Figures S11 and S12). The similarities between the genetic contexts of both families, along with their closer phylogenetic proximity in comparison to *Shewanellaceae* species (Figure S9), suggest that the potential insertion into *Geobacteraceae* genomes might have originated from horizontal transmission from a member of the *Desulfovibrionaceae* family or closely related species.

3.3.4. Inner-Membrane Quinone Oxidoreductase Protein Complexes: CbcC and CbcT Subunits Provide Plasticity and Modularity to Different Complexes Involved in EET

Cytochrome bc1 complexes are membrane protein complexes found in the electron transfer chains of bacteria using oxygen, nitrogen, and sulfur compounds as electron acceptors. These enzymes transfer electrons from ubiquinol to cytochrome c and move protons across the membrane. Despite transcriptomic and proteomic studies revealing differential expression patterns of Cbc-like gene clusters in *G. sulfurreducens* in response to electron acceptor availability, there is still limited information available regarding these complexes [237,244,299,300].

CbcT homologs are present in high abundance across all three families. In the *Desulfovibrionaceae* family, which has the highest average number of cbcT homologs (9.8), *Pseudo-*

desulfovibrio mercurii is noteworthy with 17 copies (Tables S2 and S6). *G. uraniireducens* Rf4 and *S. sediminis* HAW-EB3, from the *Geobacteraceae* and *Shewanellaceae* families, respectively, stand out with the largest numbers of CbcT orthologs, at 11 and 19 genes, respectively, except for *S. denitrificans*, which does not contain these genes. The intricate topology of the phylogenetic tree mirrors the abundance of this gene. Specifically, distinguishing clades by family is challenging due to their phylogenetically interwoven sequences. Moreover, there does not appear to be a relationship between abundance and sources of isolation, as the amount varies across all environmental classifications (Figure S9).

The cbcSTU operon is highly conserved among *Geobacteraceae* species (Figure S12). Among the strains analyzed, only *Geobacter* sp. FeAm09 presents homologs of cbcT, but neither cbcS not cbcU. Several *Shewanellaceae* strains exhibit a closely related cluster, featuring an orthologous of cbcT, which is a homolog to the sirC gene in *S. oneidensis* MR-1. SirC is a 4Fe-4S ferredoxin that, together with its partner SirD, encoding an NrfD/PsrC-type quinol dehydrogenase, has the ability to transfer electrons from quinols to the same respiratory pathways as CymA, except for nitrate. As a consequence, this quinol dehydrogenase complex (SirCD) can functionally replace CymA in the respiratory pathways for fumarate, DMSO, and ferric citrate as the electron acceptor [301]. It is worth noting that in most of the *Shewanellaceae* strains, there are two genes adjacent to one of the homologous cbcT genes. These two genes do not have homology to cbcS and cbcU but share the same annotation as the latter two genes, and are arranged in a similar spatial disposition. Specifically, the gene encoding the cytochrome c3 family protein (similar to CbcS) is homologous to the outer-membrane lipoprotein *c*-type cytochrome OmcI in *G. sulfurreducens* PCA. In this case, similar to the cbcU gene in *G. sulfurreducens*, there is a gene encoding a cytochrome c nitrite reductase subunit NrfD, although it does not belong to the CbcU orthogroup. These observations suggest a convergent evolution event in forming these modular membrane complexes, which appear to function similarly in electron transfer from the quinol pool in different respiratory pathways [302,303]. Interestingly, *S. sediminis* HAW-EB3, which presents the greatest number of cbcT homologs (and which acquired a ppcA homolog), also presents a high number of copies of other genes involved in EET mechanisms, including cbcA/omcI (12) and mrtA (12) homologs. This strain, isolated from an unexploded ordnance dumping site in the Atlantic Ocean near Halifax Harbour, Nova Scotia, Canada, can degrade RDX, nitrate, and nitrite. However, it does not demonstrate a reduction in Fe(III) or elemental sulfur [291]. These distinctive characteristics are likely a result of the environmental pressures in its natural habitat, which gives it unique features compared to other species. Furthermore, these observations suggest that these proteins are not limited to iron- or sulfur-reduction pathways from natural sources, but to other compounds, including chemicals from industrial activity and pollution events, to which bacteria have had to adapt. Considering its genetic features, it would be interesting to conduct a more in-depth characterization to investigate the functional potential of these mechanisms. In contrast, *S. violacea* DSS12 and *S. denitrificans* OS217 either lack or have only one homolog of cbcT. These strains also lack other crucial genes involved in EET mechanisms, such as OmcA, CctA, FccA, and the MtrCAB complexes. Recently, Baker et al. (2021) also reported the absence of this last complex in both species and attributed it to an environmental pressure effect, which was linked to the transition to an aerobic environment, facilitated by their habitat at the oxygenated sediment-water interface [59,304,305]

Regarding the *Desulfovibrionaceae* family, 24 of the 42 strains analyzed contain at least one homolog of cbcC. This distinct group forms a well-differentiated clade that exhibits significant evolutionary divergence from *Geobacteraceae* and *Shewanellaceae*, suggesting adaptation to the metabolic needs of these bacteria since their last common ancestor. In fact, this group of cbcC homologs coincides with one of the clusters of the multi-heme cytochrome similarity network (Figure 3B), specifically community N#37. This cluster comprises cytochrome *c* family proteins with 10 heme motifs, forming a separate cluster from other nodes in the network, thereby supporting the observed evolutionary divergence in the phylogenetic tree. Notably, in these species, at least one of the cbcC homologs was

found alongside the rnfABCDGE operon, which was initially identified in *Rhodobacter capsulatus* [306]. The RNF complex is composed of six subunits, including four membrane proteins (RnfA, RnfD, RnfE, and RnfG) and two iron–sulfur proteins (RnfB and RnfC), and encodes a membrane-bound NADH:ferredoxin dehydrogenase [306]. Our results revealed that many members of the *Desulfovibrionaceae* family exhibit the loss of the rnfB gene and instead have a gene encoding an FAD-dependent oxidoreductase at the end of the operon (Figure 9). In the Bacteroidota/Chlorobiota group, the loss of the rnfB gene has been documented, along with the recruitment of a reductase subunit from aromatic monooxygenases (AMOr protein), resulting in the emergence of the sodium-dependent NADH:ubiquinone oxidoreductase (Na^+-NQR). This complex is commonly associated with the aerobic respiratory metabolism of pathogenic bacteria. A key distinction between Rnf and Na^+-NQR is the mechanism of electron incorporation into the complex, suggesting an alternative mechanism for electron transfer in the presence of this oxidoreductase in the Rnf complex in *Desulfovibrionaceae* family strains [307]. The presence of this oxidoreductase in the Rnf complex in strains of the *Desulfovibrionaceae* family may indicate an alternative mechanism for electron transfer. Interestingly, the strains exhibiting this substitution are typically found in marine or impacted environments, which are known for their harsh conditions compared to the habitats of strains with the RnfB subunit (mainly found in soil, animals, and freshwater). These findings imply that environmental factors such as oxygen levels and the presence of metallic and organic electron acceptors or donors may have driven the modification of the rnf operon.

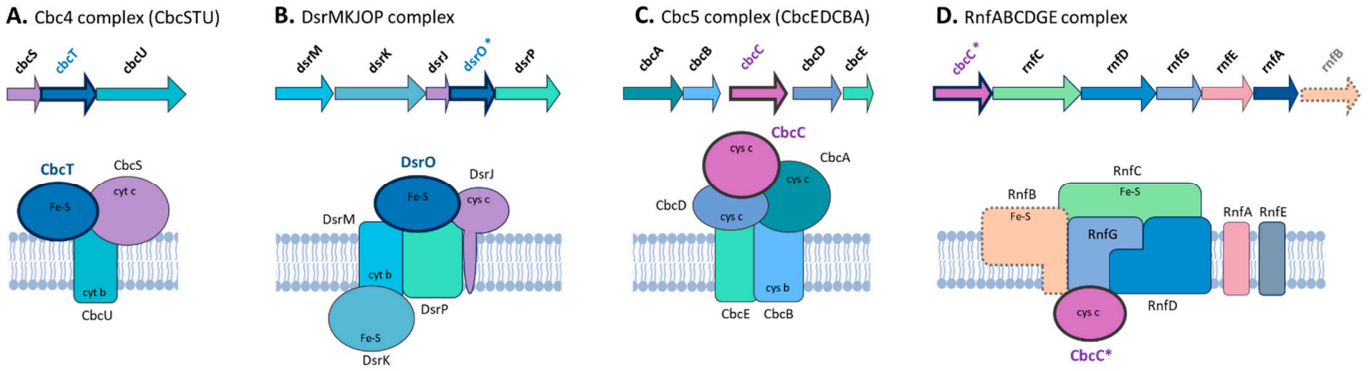

Figure 9. Schematic representation of membrane-bound complexes Cbc4, Dsr, Cbc5 and Rnf involved in EET. Gene contexts and depictions of membrane-associated complexes: (**A**) The Cbc4 complex (cbcSTU) identified in *G. sulfurreducens* PCA, consists of three subunits: a *b*-type cytochrome CbcU, an iron–sulfur cluster-binding protein CbcT, and a *c*-type cytochrome CbcS; (**B**) The Dsr complex (DsrMKJOP) in family *Desulfovibrionaceae* members, comprised of five subunits: a *b*-type cytochrome DsrM, an iron-sulfur binding protein DsrK; a triheme *c*-type cytochrome DsrJ; a ferredoxin-like protein DsrO (homologous to CbcT), and an NrfD/PsrC family integral membrane protein DsrP. The orthologous proteins CbcT from the Cbc4 complex and DsrO from the Dsr complex are highlighted in blue. (**C**) The Cbc5 complex (cbcEDCBA) from *Geobacter* species, composed of five subunits: three *c*-type cytochromes CbcA, CbcC and CbcD, a *b*-type cytochrome CbcB, and a membrane protein CbcE; and (**D**) The Rnf complex (rnfABCDGE) consists of six subunits, including four membrane proteins RnfA, RnfD, RnfE, and RnfG and two iron-sulfur proteins, RnfB and RnfC. The protein homologous to CbcC (CbcC*) is shown on the cytoplasmic side, which is possibly recruited by the Rnf complex for its function. The orthologous proteins CbcC from the Cbc5 complex and Cbc* from the Rnf complex are highlighted in violet. The rnfB subunit is indicated with dashed lines to denote its variable presence in the Rnf operon of *Desulfovibrionaceae* family. The complexes are depicted within the inner membrane, with the periplasm located at the top and the cytoplasm at the bottom.

It is important to note that in almost all strains of the *Desulfovibrionaceae* family that do not have *cbcC* homologs, the other subunits of the Rnf complex are also missing. This supports a hypothesis regarding the integration of the CbcC homolog as an accessory protein

within the complex. The only exceptions are *Desulfovibrio cuneatus* DSM 11391, which possesses the *rnf* operon minus the RnfB subunit and the CbcC homolog, and *Halodesulfovibrio aestuarii* DSM 17919, which harbors the complete *rnf* operon and a cytochrome c, not homologous to CbcC (Figure S14). All other strains with the *rnf* operon contain the *cbcC* homolog, likely indicating an ancient evolutionary incorporation event before these species diverged. Furthermore, the sporadic occurrence of this complex in some family members strongly suggests horizontal gene transfer as a mode of acquisition. Previous research indeed indicates the spread of this complex among various lineages by HGT, including several species within the phyla *Pseudomonadota*, *Chlamydiota*, and *Planctomycetota*, which subsequently led to the rise in other complexes, such as Na^+-NQR mentioned above [308]. In this context, the CbcC-like cytochrome represents a unique module that has become integrated into various membrane complexes involved in electron transfer through evolution and species diversification. In *Geobacter*, it is part of the CbcEDCBA cluster where it is predicted to form menaquinol:ferricytochrome c oxidoreductase [237], and in *Desulfovibrionaceae* family members, it forms part of the Rnf complex, with a predicted cytoplasmic location, where it likely engages in coupling to facilitate efficient electron transfer (Figure 9). These findings indicate that this subunit, adapted by *Desulfovibrionaceae* family members with significant evolutionary divergence, might offer a potential new catalytic innovation. By incorporating it into the Rnf complex, these bacteria could potentially broaden the detection of redox potentials and access an alternative electron transfer pathway, thereby enhancing growth efficiency in variable environments.

4. Implications

The coexistence of sulfate- and iron-reducing bacteria can be found in several environments with limited oxygen availability and varying redox conditions, such as marine sediments, anoxic soils, and groundwater. These bacteria have developed mechanisms for utilizing external electron donors and acceptors for energy metabolism, including EET. However, the distribution, diversity, and evolution of the EET mechanisms are still not well understood, and the underlying molecular mechanisms shared between SRB and FeRB remain unexplored. In this study, a comparative genomic analysis uncovered the similarities and differences in the distribution of genes related to EET in the genomes of the *Desulfovibrionaceae*, *Geobacteraceae*, and *Shewanellaceae* families. Our results showed a higher abundance of multi-heme cytochromes, especially those that were extracellular, in *Geobacteraceae* strains than *Desulfovibrionaceae* and *Shewanellaceae.* The analysis also showed more orthologous groups (OGs) shared between these two families than *Geobacteraceae*, suggesting a closer phylogenomic relationship. However, this did not necessarily correlate with OGs related to EET. In fact, the strains belonging to *Desulfovibrionaceae* shared more homologous genes related to EET with the model *G. sulfurreducens* PCA compared to *S. oneidensis* MR-1.

Within each family, a set of genes related to EET proteins exhibited significant enrichment. For example, the presence of gene copies encoding CymA and riboflavins distinguished *Shewanellaceae*, while those encoding OmpJ differentiated the *Desulfovibrionaceae*. Similarly, the presence of gene copies encoding Cbc and total cytochromes distinguished the *Geobacteraceae* from other families. After conducting a comprehensive analysis, we identified potential horizontal gene transfer events, gene gain or loss events, and instances of convergent evolution related to specific proteins. These findings enhance our understanding of the distribution and evolution of EET genes and pathways across diverse phylogenetic groups of SRB and FeRB. These discoveries contribute to our understanding of the adaptability of these bacteria and their diverse electron transfer pathways in different environments, especially relevant in environments with redox gradients.

Supplementary Materials: The following supporting information can be downloaded at: https://www.mdpi.com/article/10.3390/microorganisms12091796/s1, Table S1: Genomic features of the SRB and FeRB genomes; Table S2: Custom database for EET-related genes belonging to the *Desulfovibrionaceae*, *Geobacteraceae*, and *Shewanellaceae* families; Table S3: Growth conditions of SRB and FeRB genomes; Table S4: Mobilome-related counts found in the genomes of SRB and FeRB genomes; Table S5: Prevalence of mobilome elements in the genomes of SRB and FeRB genomes; Table S6: Counts of c-type cytochromes found in the genomes of SRB and FeRB genomes; Table S7: References of growth conditions of SRB and FeRB genomes; Figure S1: Orthology analysis of the SRB and FeRB genomes. (A) Number of orthogroups (OGs) versus the number of genomes in log10 scale. The first (left) and last (right) bars represent the species-specific OGs (546) and the core OGs with all species present (289), respectively. (D) Venn diagram showing unique and shared ortholog gene clusters in the three families. The number of unassigned genes to OGs is shown in parentheses. Figure S2: Phylogenomic tree of the analyzed genomes belonging to the *Desulfovibrionaceae*, *Geobacteraceae*, and *Shewanellaceae* families. Phylogeny was inferred using Orthofinder v2.5.4, identifying 109 single-copy orthogroups with all species present. (A) Clades of each family, (B), (C), and (D) show the subclades of strains belonging to *Desulfovibrionaceae*, *Geobacteraceae*, and *Shewanellaceae* families, respectively; Figure S3: Violin-plots of the distribution of (A) genomic GC content and (B) genome size by subclades of *Desulfovibrionaceae*, *Geobacteraceae*, and *Shewanellaceae* families; Figure S4: Presence/absence matrix of genes of complementary genes related to EET mechanisms of *S. oneidensis* MR-1 y *G. sulfurreducens* PCA. On the left, the phylogenomic cladogram is presented with the isolation source according to Figure 1; Figure S5: Correlation between prophage density (total number of prophages per Mbp) and the average total prophages per strain found in each family; Figure S6: Principal Component Analysis of the strains from the *Desulfovibrionaceae*, *Geobacteraceae* and *Shewanellaceae* families in relation to their mobilome components, types of cytochromes, genome size, and GC content. Colors indicate strains origin/habitat; Figure S7: Phylogeny and genetic context of PpcA orthologous proteins. The phylogenetic tree was constructed using MrBayes method based on amino acid sequences of 64 proteins, 40 belonging to members of *Desulfovibrionaceae* family, 22 belonging to *Geobacteraceae* family and two belonging to *Shewanellaceae* family. Bayesian posterior probabilities are indicated above their branch. The scale bar shows 0.3 estimated substitutions per site. The tree was rooted to the closest protein of *Thermovibrio ammonificans* HB-1. The number before the bacterial name indicates the position with respect to the phylogenomic tree (obtained with Orthofinder). Colors next to the phylogenetic tree indicate the source of isolation: blue for marine waters/sediments, turquoise for brackish water/sediments, cyan for freshwater sediments, purple for engineered/impacted system, green for plant/algae-associated, orange for animal/human-associated, yellow for soil, red for food, and gray for unknown source. The blue triangles indicate those bacteria from *Desulfovibrionaceae* family that have reported Fe(III) reduction. On the right, the genetic contexts of the *ppcA* orthologous genes are visualized. The lower zone shows the genetic context of the gene encoding the periplasmic cytochrome ppcA of *Geobacter sulfurreducens* PCA; Figure S8: Genetic context of *ppcA*-orthologous genes in others representative strains of the *Desulfovibrionaceae* family. Genetic context of *ppcA* gene of (A) *Maridesulfovibrio frigidus* DSM 17176 (WP_031480636.1), (B) *Desulfocurvibacter africanus* PCS (WP_005987327.1), (C) *Desulfovibrio vulgaris* Hildenborough (WP_010940429.1), and (D) *Desulfovibrio desulfuricans* DSM 642 (WP_022659815.1); Figure S9: Phylogenetic trees of the orthologous groups associated with OmpJ, CymA, CbcT and CbcC. The phylogenetic trees were inferred using Orthofinder v2.5.4. (A) Phylogenetic tree of proteins homologous of the outer membrane protein OmpJ. The tree comprises 225 protein sequences: 42 from *Geobacter* strains and 183 from members of the *Desulfovibrionaceae* family. (B) Phylogenetic tree of proteins homologous of the c-type cytochrome CymA. The tree is composed of 232 protein sequences: 17 from *Geobacter* strains, 162 from *Shewanella* and 53 from members of the *Desulfovibrionaceae* family. (C) Phylogenetic tree of proteins homologous of the cytochrome bc complex CbcT. The tree is composed of 1018 protein sequences: 161 from *Geobacter* strains, 447 from *Shewanella* and 410 from members of the *Desulfovibrionaceae* family. (D) Phylogenetic tree of proteins homologous of the cytochrome bc complex CbcC. The tree is composed of 136 protein sequences: 94 from *Geobacter* strains, 4 from *Shewanella* and 38 from members of the *Desulfovibrionaceae* family. Each clade/branch is colored according to its family of origin; Figure S10: Phylogeny and genetic context of OmpJ orthologous proteins. The phylogenetic tree was constructed using MrBayes method based on amino acid sequences of 64 proteins, 42 belonging to members of *Desulfovibrionaceae* family and 22 belonging to *Geobacteraceae* family. Bayesian posterior probabilities are indicated above their branch. The scale bar shows 0.3 estimated substitutions per site. The tree was rooted to the

closest protein of *Thermovibrio ammonificans* HB-1. The number before the bacterial name indicates the position with respect to the phylogenomic tree (obtained with Orthofinder). Colors next to the phylogenetic tree indicate the source of isolation: blue for marine waters/sediments, turquoise for brackish water/sediments, cyan for freshwater sediments, purple for engineered/impacted system, green for plant/algae-associated, orange for animal/human-associated, yellow for soil, red for food, and gray for unknown source. The blue triangles indicate those bacteria from *Desulfovibrionaceae* family that have reported Fe(III) reduction. On the right, the genetic contexts of the *ompJ* orthologous genes are visualized. The bottom of the figure shows the genetic context of the gene encoding the outer membrane protein OmpJ of *Geobacter sulfurreducens* PCA; Figure S11: Phylogeny and genetic context of CymA orthologous proteins. The phylogenetic tree was constructed using MrBayes method based on amino acid sequences of 113 proteins, 40 belonging to members of *Desulfovibrionaceae* family, 14 to *Geobacteraceae* family and 59 belonging to *Shewanellaceae* family. Bayesian posterior probabilities are indicated above their branch. The scale bar shows 0.3 estimated substitutions per site. The tree was rooted to the closest protein of *Thermovibrio ammonificans* HB-1. The number before the bacterial name indicates the position with respect to the phylogenomic tree (obtained with Orthofinder). Colors next to the phylogenetic tree indicate the source of isolation: blue for marine waters/sediments, turquoise for brackish water/sediments, cyan for freshwater sediments, purple for engineered/impacted system, green for plant/algae-associated, orange for animal/human-associated, yellow for soil, red for food, and gray for unknown source. The blue triangles indicate those bacteria from *Desulfovibrionaceae* family that have reported Fe(III) reduction. On the right, the genetic contexts of the *cymA* orthologous genes are visualized. The lower zone shows the genetic context of the gene encoding the tetraheme c-type cytochrome CymA of *Shewanella oneidensis MR-1*; Figure S12: Genetic context of *cymA*-orthologous genes in others representative strains of the *Desulfovibrionaceae* family. Genetic context of *cymA* gene of (A) *Maridesulfovibrio frigidus* DSM 17176 (WP_031480646.1), (B) *Desulfocurvibacter africanus* PCS (WP_005984200.1), (C) *Desulfovibrio vulgaris* Hildenborough (WP_010937927.1), and (D) *Desulfovibrio desulfuricans* DSM 642 (WP_022659018.1); Figure S13: Phylogeny and genetic context of CbcT orthologous proteins. The phylogenetic tree was constructed using MrBayes method based on amino acid sequences of 72 proteins, 42 belonging to members of *Desulfovibrionaceae* family, and 30 representative sequences of the *Geobacteraceae* and *Shewanellaceae* families (10 and 20, respectively). Bayesian posterior probabilities are indicated above their branch. The scale bar shows 0.2 estimated substitutions per site. The tree was rooted to the closest protein of *Thermovibrio ammonificans* HB-1. The number before the bacterial name indicates the position with respect to the phylogenomic tree (obtained with Orthofinder). Colors next to the phylogenetic tree indicate the source of isolation: blue for marine waters/sediments, turquoise for brackish water/sediments, cyan for freshwater sediments, purple for engineered/impacted system, green for plant/algae-associated, orange for animal/human-associated, yellow for soil, red for food, and gray for unknown source. The blue triangles indicate those bacteria from *Desulfovibrionaceae* family that have reported Fe(III) reduction. On the right, the genetic contexts of the *cbcT* orthologous genes are visualized. The lower zone shows the genetic context of the gene encoding the iron-sulfur cluster-binding protein CbcT of *Geobacter sulfurreducens* PCA. CbcT, together with c-type cytochrome CbcS and b-type cytochrome CbcU represent the menaquinol: ferricytochrome c oxidoreductase complex; Figure S14: Phylogeny and genetic context of CbcC orthologous proteins. The phylogenetic tree was constructed using MrBayes method based on amino acid sequences of 50 proteins, 24 belonging to members of *Desulfovibrionaceae* family, 22 to *Geobacteraceae* family and 4 belonging to *Shewanellaceae* family. Bayesian posterior probabilities are indicated above their branch. The scale bar shows 0.4 estimated substitutions per site. The tree was rooted to the closest protein of *Thermovibrio ammonificans* HB-1. The number before the bacterial name indicates the position with respect to the phylogenomic tree (obtained with Orthofinder). Colors next to the phylogenetic tree indicate the source of isolation: blue for marine waters/sediments, turquoise for brackish water/sediments, cyan for freshwater sediments, purple for engineered/impacted system, green for plant/algae-associated, orange for animal/human-associated, yellow for soil, red for food, and gray for unknown source. The blue triangles indicate those bacteria from *Desulfovibrionaceae* family that have reported Fe(III) reduction. On the right, the genetic contexts of the *cbcC* orthologous genes are visualized. The lower zone shows the genetic context of the gene encoding the c-type cytochrome CbcC of *Geobacter sulfurreducens* PCA. CbcC is part of the Cbc5 complex (cbcEDCBA), a menaquinol:ferricytochrome c oxidoreductase complex, expressed during the reduction of Fe(III) oxide minerals; Figure S15: Multi-heme cytochrome similarity networking. Similarity network colored according to: (A) Isolation

source of the bacteria of origin; (B) Salt tolerance level of the bacteria; (C) Experimental evidence of Fe(III) reduction of the bacteria and; (D) Classification according to OGs, in color are shown some more abundant OGs (8/35).

Author Contributions: Conceptualization, V.G., A.A. and R.O.; Methodology, J.A.-H., M.R.G. and R.O.; Validation, V.G. and J.A.-H.; Formal analysis, V.G., A.A. and M.R.G.; Investigation, V.G., J.A.-H., A.A., F.C., M.R.G. and R.O.; Resources, R.O.; Data curation, V.G., J.A.-H. and F.C.; Writing—original draft, V.G., J.A.-H. and R.O.; Writing—review & editing, V.G., A.A. and R.O.; Visualization, V.G. and J.A.-H.; Project administration, A.A.; Funding acquisition, A.A. and R.O. All authors have read and agreed to the published version of the manuscript.

Funding: This study was supported by the "Agencia Nacional de Investigación y Desarrollo (ANID)", through Fondecyt de Iniciación #11190863 ("Meet MEET (Microbial Extracellular Electron Transfer) in Sulfidogenic Environments: New Views of an Old Cycle"), Fondecyt Regular #1211977 ("Methane and ammonia oxidation interactions and their effect on greenhouse gases in ecosystems with diverse methane and nitrogen sources"), Programa de Inserción a la Academia PAI79170091, Project ANID-FOVI 230154 ("Fortalecimiento de red de colaboración para el estudio y caracterización de microorganismos electroquímicamente activos"), Plan de Fortalecimiento Universidades Estatales-Ministerio de Educación, Convenio UPA 1999, and ANID-Milenio-NCN2023_054. J.A-H. was supported by ANID Scholarship 21231799/.2023.

Data Availability Statement: Data are contained within the article.

Conflicts of Interest: The authors declare no conflict of interest.

References

1. Bao, P.; Li, G.X.; Sun, G.X.; Xu, Y.Y.; Meharg, A.A.; Zhu, Y.G. The role of sulfate-reducing prokaryotes in the coupling of element biogeochemical cycling. *Sci. Total Environ.* **2018**, *613–614*, 398–408. [CrossRef] [PubMed]
2. Yu, S.-S.; Chen, J.-J.; Cheng, R.-F.; Min, Y.; Yu, H.-Q. Iron Cycle Tuned by Outer-Membrane Cytochromes of Dissimilatory Metal-Reducing Bacteria: Interfacial Dynamics and Mechanisms In Vitro. *Environ. Sci. Technol.* **2021**, *55*, 11424–11433. [CrossRef]
3. Wunder, L.C.; Aromokeye, D.A.; Yin, X.; Richter-Heitmann, T.; Willis-Poratti, G.; Schnakenberg, A.; Otersen, C.; Dohrmann, I.; Römer, M.; Bohrmann, G.; et al. Iron and sulfate reduction structure microbial communities in (sub-)Antarctic sediments. *ISME J.* **2021**, *15*, 3587–3604. [CrossRef]
4. Berg, J.S.; Jézéquel, D.; Duverger, A.; Lamy, D.; Laberty-Robert, C.; Miot, J. Microbial diversity involved in iron and cryptic sulfur cycling in the ferruginous, low-sulfate waters of Lake Pavin. *PLoS ONE* **2019**, *14*, e0212787. [CrossRef] [PubMed]
5. Hu, K.; Xu, D.; Chen, Y. An assessment of sulfate reducing bacteria on treating sulfate-rich metal-laden wastewater from electroplating plant. *J. Hazard. Mater.* **2020**, *393*, 122376. [CrossRef] [PubMed]
6. Kovacik, W.P., Jr.; Takai, K.; Mormile, M.R.; McKinley, J.P.; Brockman, F.J.; Fredrickson, J.K.; Holben, W.E. Molecular analysis of deep subsurface Cretaceous rock indicates abundant Fe(III)- and S°-reducing bacteria in a sulfate-rich environment. *Environ. Microbiol.* **2006**, *8*, 141–155. [CrossRef] [PubMed]
7. Muyzer, G.; Stams, A.J.M. The ecology and biotechnology of sulphate-reducing bacteria. *Nat. Rev. Microbiol.* **2008**, *6*, 441–454. [CrossRef]
8. Rey, F.E.; Gonzalez, M.D.; Cheng, J.; Wu, M.; Ahern, P.P.; Gordon, J.I. Metabolic niche of a prominent sulfate-reducing human gut bacterium. *Proc. Natl. Acad. Sci. USA* **2013**, *110*, 13582–13587. [CrossRef]
9. Reyes, C.; Dellwig, O.; Dähnke, K.; Gehre, M.; Noriega-Ortega, B.E.; Böttcher, M.E.; Meister, P.; Friedrich, M.W. Bacterial communities potentially involved in iron-cycling in Baltic Sea and North Sea sediments revealed by pyrosequencing. *FEMS Microbiol. Ecol.* **2016**, *92*, fiw054. [CrossRef]
10. Buongiorno, J.; Herbert, L.C.; Wehrmann, L.M.; Michaud, A.B.; Laufer, K.; Røy, H.; Jørgensen, B.B.; Szynkiewicz, A.; Faiia, A.; Yeager, K.M.; et al. Complex Microbial Communities Drive Iron and Sulfur Cycling in Arctic Fjord Sediments. *Appl. Environ. Microbiol.* **2019**, *85*, e00949-19. [CrossRef]
11. Chapelle, F.H.; Lovley, D.R. Competitive Exclusion of Sulfate Reduction by Fe(lll)-Reducing Bacteria: A Mechanism for Producing Discrete Zones of High-Iron Ground Water. *Groundwater* **1992**, *30*, 29–36. [CrossRef]
12. Ayangbenro, A.S.; Olanrewaju, O.S.; Babalola, O.O. Sulfate-Reducing Bacteria as an Effective Tool for Sustainable Acid Mine Bioremediation. *Front. Microbiol.* **2018**, *9*, 1986. [CrossRef] [PubMed]
13. Canfield, D.E.; Jørgensen, B.B.; Fossing, H.; Glud, R.; Gundersen, J.; Ramsing, N.B.; Thamdrup, B.; Hansen, J.W.; Nielsen, L.P.; Hall, P.O.J. Pathways of organic carbon oxidation in three continental margin sediments. *Mar. Geol.* **1993**, *113*, 27–40. [CrossRef]
14. Canfield, D.E.; Thamdrup, B.; Hansen, J.W. The anaerobic degradation of organic matter in Danish coastal sediments: Iron reduction, manganese reduction, and sulfate reduction. *Geochim. Cosmochim. Acta* **1993**, *57*, 3867–3883. [CrossRef]
15. Xing, C.; Lang, X.; Ma, H.; Peng, Y.; Peng, Y.; Liu, Y.; Wang, R.; Ning, M.; Cui, Y.; Yu, X.; et al. Predominant microbial iron reduction in sediment in early Cambrian sulfidic oceans. *Glob. Planet. Chang.* **2021**, *206*, 103637. [CrossRef]

16. Bowles, M.W.; Mogollón, J.M.; Kasten, S.; Zabel, M.; Hinrichs, K.-U. Global rates of marine sulfate reduction and implications for sub–sea-floor metabolic activities. *Science* **2014**, *344*, 889–891. [CrossRef]
17. Dong, H.; Zeng, Q.; Sheng, Y.; Chen, C.; Yu, G.; Kappler, A. Coupled iron cycling and organic matter transformation across redox interfaces. *Nat. Rev. Earth Environ.* **2023**, *4*, 659–673. [CrossRef]
18. Plugge, C.; Zhang, W.; Scholten, J.; Stams, A. Metabolic Flexibility of Sulfate-Reducing Bacteria. *Front. Microbiol.* **2011**, *2*, 81. [CrossRef]
19. Jørgensen, B.B. Mineralization of organic matter in the sea bed—The role of sulphate reduction. *Nature* **1982**, *296*, 643–645. [CrossRef]
20. Jørgensen, B.B.; Kasten, S. Sulfur Cycling and Methane Oxidation. In *Marine Geochemistry*; Schulz, H.D., Zabel, M., Eds.; Springer: Berlin/Heidelberg, Germany, 2006; pp. 271–309.
21. Fike, D.A.; Bradley, A.S.; Rose, C.V. Rethinking the Ancient Sulfur Cycle. *Annu. Rev. Earth Planet. Sci.* **2015**, *43*, 593–622. [CrossRef]
22. Raven, M.R.; Keil, R.G.; Webb, S.M. Microbial sulfate reduction and organic sulfur formation in sinking marine particles. *Science* **2021**, *371*, 178–181. [CrossRef]
23. Lovley, D.R.; Holmes, D.E.; Nevin, K.P. Dissimilatory Fe(III) and Mn(IV) reduction. *Adv. Microb. Physiol.* **2004**, *49*, 219–286. [CrossRef] [PubMed]
24. Jickells, T.D.; An, Z.S.; Andersen, K.K.; Baker, A.R.; Bergametti, G.; Brooks, N.; Cao, J.J.; Boyd, P.W.; Duce, R.A.; Hunter, K.A.; et al. Global iron connections between desert dust, ocean biogeochemistry, and climate. *Science* **2005**, *308*, 67–71. [CrossRef]
25. Champ, D.; Gulens, J.; Jackson, R. Oxidation-Reduction Sequences in Ground Water Flow Systems. *Can. J. Earth Sci.* **2011**, *16*, 12–23. [CrossRef]
26. Lovley, D.R.; Chapelle, F.H.; Woodward, J.C. Use of Dissolved H_2 Concentrations To Determine Distribution of Microbially Catalyzed Redox Reactions in Anoxic Groundwater. *Environ. Sci. Technol.* **1994**, *28*, 1205–1210. [CrossRef] [PubMed]
27. Bethke, C.; Sanford, R.; Kirk, M.; Jin, Q.; Flynn, T. The Thermodynamic ladder in Geomicrobiology. *Am. J. Sci.* **2011**, *311*, 183–210. [CrossRef]
28. Lovley, D.R.; Goodwin, S. Hydrogen concentrations as an indicator of the predominant terminal electron-accepting reactions in aquatic sediments. *Geochim. Cosmochim. Acta* **1988**, *52*, 2993–3003. [CrossRef]
29. Lovley, D.R.; Phillips, E.J.P. Competitive Mechanisms for Inhibition of Sulfate Reduction and Methane Production in the Zone of Ferric Iron Reduction in Sediments. *Appl. Environ. Microbiol.* **1987**, *53*, 2636–2641. [CrossRef]
30. Kirk, M.F.; Jin, Q.; Haller, B.R. Broad-Scale Evidence That pH Influences the Balance Between Microbial Iron and Sulfate Reduction. *Groundwater* **2016**, *54*, 406–413. [CrossRef]
31. Canfield, D.E.; Erik, K.; Bo, T. Thermodynamics and Microbial Metabolism. In *Advances in Marine Biology*; Canfield, D.E., Kristensen, E., Thamdrup, B., Eds.; Academic Press: Cambridge, MA, USA, 2005; Volume 48, pp. 65–94.
32. Kappler, A.; Bryce, C.; Mansor, M.; Lueder, U.; Byrne, J.M.; Swanner, E.D. An evolving view on biogeochemical cycling of iron. *Nat. Rev. Microbiol.* **2021**, *19*, 360–374. [CrossRef]
33. Jørgensen, B.B.; Findlay, A.J.; Pellerin, A. The Biogeochemical Sulfur Cycle of Marine Sediments. *Front. Microbiol.* **2019**, *10*, 849. [CrossRef]
34. Sinninghe Damst'e, J.S.; Rijpstra, W.I.C.; Kock-van Dalen, A.C.; De Leeuw, J.W.; Schenck, P.A. Quenching of labile functionalised lipids by inorganic sulphur species: Evidence for the formation of sedimentary organic sulphur compounds at the early stages of diagenesis. *Geochim. Cosmochim. Acta* **1989**, *53*, 1343–1355. [CrossRef]
35. Yu, Z.-G.; Peiffer, S.; Göttlicher, J.; Knorr, K.-H. Electron Transfer Budgets and Kinetics of Abiotic Oxidation and Incorporation of Aqueous Sulfide by Dissolved Organic Matter. *Environ. Sci. Technol.* **2015**, *49*, 5441–5449. [CrossRef] [PubMed]
36. Heitmann, T.; Blodau, C. Oxidation and incorporation of hydrogen sulfide by dissolved organic matter. *Chem. Geol.* **2006**, *235*, 12–20. [CrossRef]
37. Froelich, P.N.; Klinkhammer, G.P.; Bender, M.L.; Luedtke, N.A.; Heath, G.R.; Cullen, D.; Dauphin, P.; Hammond, D.; Hartman, B.; Maynard, V. Early oxidation of organic matter in pelagic sediments of the eastern equatorial Atlantic: Suboxic diagenesis. *Geochim. Cosmochim. Acta* **1979**, *43*, 1075–1090. [CrossRef]
38. Hoehler, T.M.; Alperin, M.J.; Albert, D.B.; Martens, C.S. Thermodynamic control on hydrogen concentrations in anoxic sediments. *Geochim. Cosmochim. Acta* **1998**, *62*, 1745–1756. [CrossRef]
39. Coleman, M.L.; Hedrick, D.B.; Lovley, D.R.; White, D.C.; Pye, K. Reduction of Fe(III) in sediments by sulphate-reducing bacteria. *Nature* **1993**, *361*, 436–438. [CrossRef]
40. Ke, C.; Guo, C.; Zhang, S.; Deng, Y.; Li, X.; Li, Y.; Lu, G.; Ling, F.; Dang, Z. Microbial reduction of schwertmannite by co-cultured iron- and sulfate-reducing bacteria. *Sci. Total Environ.* **2023**, *861*, 160551. [CrossRef] [PubMed]
41. Lovley, D.R.; Roden, E.E.; Phillips, E.J.P.; Woodward, J.C. Enzymatic iron and uranium reduction by sulfate-reducing bacteria. *Mar. Geol.* **1993**, *113*, 41–53. [CrossRef]
42. Holmes, D.E.; Bond, D.R.; Lovley, D.R. Electron transfer by *Desulfobulbus propionicus* to Fe(III) and graphite electrodes. *Appl. Environ. Microbiol.* **2004**, *70*, 1234–1237. [CrossRef] [PubMed]
43. Park, H.S.; Lin, S.; Voordouw, G. Ferric iron reduction by *Desulfovibrio vulgaris* Hildenborough wild type and energy metabolism mutants. *Antonie Van Leeuwenhoek* **2008**, *93*, 79–85. [CrossRef] [PubMed]
44. Dalla Vecchia, E.; Shao, P.P.; Suvorova, E.; Chiappe, D.; Hamelin, R.; Bernier-Latmani, R. Characterization of the surfaceome of the metal-reducing bacterium *Desulfotomaculum reducens*. *Front. Microbiol.* **2014**, *5*, 432. [CrossRef] [PubMed]

45. Brown, S.D.; Utturkar, S.M.; Arkin, A.P.; Deutschbauer, A.M.; Elias, D.A.; Hazen, T.C.; Chakraborty, R. Draft Genome Sequence for *Desulfovibrio africanus* Strain PCS. *Genome Announc.* **2013**, *1*, e00144-13. [CrossRef]
46. Vandieken, V.; Knoblauch, C.; Jørgensen, B.B. *Desulfovibrio frigidus* sp. nov. and *Desulfovibrio ferrireducens* sp. nov., psychrotolerant bacteria isolated from Arctic fjord sediments (Svalbard) with the ability to reduce Fe(III). *Int. J. Syst. Evol. Microbiol.* **2006**, *56*, 681–685. [CrossRef]
47. Badalamenti, J.P.; Summers, Z.M.; Chan, C.H.; Gralnick, J.A.; Bond, D.R. Isolation and Genomic Characterization of '*Desulfuromonas soudanensis* WTL', a Metal- and Electrode-Respiring Bacterium from Anoxic Deep Subsurface Brine. *Front. Microbiol.* **2016**, *7*, 913. [CrossRef]
48. Liang, D.; Liu, X.; Woodard, T.L.; Holmes, D.E.; Smith, J.A.; Nevin, K.P.; Feng, Y.; Lovley, D.R. Extracellular Electron Exchange Capabilities of *Desulfovibrio ferrophilus* and *Desulfopila corrodens*. *Environ. Sci. Technol.* **2021**, *55*, 16195–16203. [CrossRef]
49. Enning, D.; Garrelfs, J. Corrosion of iron by sulfate-reducing bacteria: New views of an old problem. *Appl. Environ. Microbiol.* **2014**, *80*, 1226–1236. [CrossRef]
50. Ueki, T.; Lovley, D.R. *Desulfovibrio vulgaris* as a model microbe for the study of corrosion under sulfate-reducing conditions. *mLife* **2022**, *1*, 13–20. [CrossRef]
51. Ayala Nuñez, T.; Cerbino, G.N.; Rapisardi, M.F.; Quiroga, C.; Centrón, D. Novel Mobile Integrons and Strain-Specific Integrase Genes within *Shewanella* spp. Unveil Multiple Lateral Genetic Transfer Events within the Genus. *Microorganisms* **2022**, *10*, 1102. [CrossRef] [PubMed]
52. Cerbino, G.N.; Traglia, G.M.; Ayala Nuñez, T.; Parmeciano Di Noto, G.; Ramírez, M.S.; Centrón, D.; Iriarte, A.; Quiroga, C. Comparative genome analysis of the genus *Shewanella* unravels the association of key genetic traits with known and potential pathogenic lineages. *Front. Microbiol.* **2023**, *14*, 1124225. [CrossRef]
53. Orellana, R.; Arancibia, A.; Badilla, L.; Acosta, J.; Arancibia, G.; Escar, R.; Ferrada, G.; Seeger, M. Ecophysiological Features Shape the Distribution of Prophages and CRISPR in Sulfate Reducing Prokaryotes. *Microorganisms* **2021**, *9*, 931. [CrossRef] [PubMed]
54. Holmes, D.E.; Giloteaux, L.; Chaurasia, A.K.; Williams, K.H.; Luef, B.; Wilkins, M.J.; Wrighton, K.C.; Thompson, C.A.; Comolli, L.R.; Lovley, D.R. Evidence of *Geobacter*-associated phage in a uranium-contaminated aquifer. *ISME J.* **2015**, *9*, 333–346. [CrossRef] [PubMed]
55. Crispim, J.S.; Dias, R.S.; Vidigal, P.M.P.; de Sousa, M.P.; da Silva, C.C.; Santana, M.F.; de Paula, S.O. Screening and characterization of prophages in *Desulfovibrio* genomes. *Sci. Rep.* **2018**, *8*, 9273. [CrossRef] [PubMed]
56. Hernández, S.; Vives, M.J. Phages in Anaerobic Systems. *Viruses* **2020**, *12*, 1091. [CrossRef]
57. Caro-Quintero, A.; Deng, J.; Auchtung, J.; Brettar, I.; Höfle, M.G.; Klappenbach, J.; Konstantinidis, K.T. Unprecedented levels of horizontal gene transfer among spatially co-occurring *Shewanella* bacteria from the Baltic Sea. *ISME J.* **2011**, *5*, 131–140. [CrossRef]
58. Zhong, C.; Han, M.; Yu, S.; Yang, P.; Li, H.; Ning, K. Pan-genome analyses of 24 *Shewanella* strains re-emphasize the diversification of their functions yet evolutionary dynamics of metal-reducing pathway. *Biotechnol. Biofuels* **2018**, *11*, 193. [CrossRef]
59. Baker, I.R.; Conley, B.E.; Gralnick, J.A.; Girguis, P.R. Evidence for Horizontal and Vertical Transmission of Mtr-Mediated Extracellular Electron Transfer among the Bacteria. *mBio* **2021**, *13*, e0290421. [CrossRef]
60. Kumar, A.; Hsu, L.H.-H.; Kavanagh, P.; Barrière, F.; Lens, P.N.L.; Lapinsonnière, L.; Lienhard, V.J.H.; Schröder, U.; Jiang, X.; Leech, D. The ins and outs of microorganism–electrode electron transfer reactions. *Nat. Rev. Chem.* **2017**, *1*, 0024. [CrossRef]
61. Shi, L.; Dong, H.; Reguera, G.; Beyenal, H.; Lu, A.; Liu, J.; Yu, H.-Q.; Fredrickson, J.K. Extracellular electron transfer mechanisms between microorganisms and minerals. *Nat. Rev. Microbiol.* **2016**, *14*, 651–662. [CrossRef]
62. Cai, X.; Huang, L.; Yang, G.; Yu, Z.; Wen, J.; Zhou, S. Transcriptomic, Proteomic, and Bioelectrochemical Characterization of an Exoelectrogen *Geobacter soli* Grown with Different Electron Acceptors. *Front. Microbiol.* **2018**, *9*, 1075. [CrossRef]
63. Antunes, J.M.A.; Silva, M.A.; Salgueiro, C.A.; Morgado, L. Electron Flow From the Inner Membrane Towards the Cell Exterior in *Geobacter sulfurreducens:* Biochemical Characterization of Cytochrome CbcL. *Front. Microbiol.* **2022**, *13*, 898015. [CrossRef] [PubMed]
64. Ueki, T. Cytochromes in Extracellular Electron Transfer in *Geobacter*. *Appl. Environ. Microbiol.* **2021**, *87*, e03109-20. [CrossRef]
65. Hau, H.H.; Gralnick, J.A. Ecology and Biotechnology of the Genus *Shewanella*. *Annu. Rev. Microbiol.* **2007**, *61*, 237–258. [CrossRef] [PubMed]
66. Parks, D.H.; Imelfort, M.; Skennerton, C.T.; Hugenholtz, P.; Tyson, G.W. CheckM: Assessing the quality of microbial genomes recovered from isolates, single cells, and metagenomes. *Genome Res.* **2015**, *25*, 1043–1055. [CrossRef] [PubMed]
67. Emms, D.M.; Kelly, S. OrthoFinder: Phylogenetic orthology inference for comparative genomics. *Genome Biol.* **2019**, *20*, 238. [CrossRef]
68. Katoh, K.; Standley, D.M. MAFFT multiple sequence alignment software version 7: Improvements in performance and usability. *Mol. Biol. Evol.* **2013**, *30*, 772–780. [CrossRef]
69. Price, M.N.; Dehal, P.S.; Arkin, A.P. FastTree 2—Approximately Maximum-Likelihood Trees for Large Alignments. *PLoS ONE* **2010**, *5*, e9490. [CrossRef] [PubMed]
70. Kumar, S.; Stecher, G.; Li, M.; Knyaz, C.; Tamura, K. MEGA X: Molecular Evolutionary Genetics Analysis across Computing Platforms. *Mol. Biol. Evol.* **2018**, *35*, 1547–1549. [CrossRef]
71. Letunic, I.; Bork, P. Interactive Tree Of Life (iTOL) v5: An online tool for phylogenetic tree display and annotation. *Nucleic Acids Res.* **2021**, *49*, W293–W296. [CrossRef]

72. Kuever, J.; Rainey, F.A.; Widdel, F. Desulfovibrio. In *Bergey's Manual of Systematics of Archaea and Bacteria*; Wiley: Hoboken, NJ, USA, 2015; pp. 1–17.
73. Campbell, L.L.; Kasprzycki, M.A.; Postgate, J.R. *Desulfovibrio africanus* sp. n., a New Dissimilatory Sulfate-reducing Bacterium. *J. Bacteriol.* **1966**, *92*, 1122–1127. [CrossRef]
74. Motamedi, M.; Pedersen, K. *Desulfovibrio aespoeensis* sp. nov., a mesophilic sulfate-reducing bacterium from deep groundwater at Äspö hard rock laboratory, Sweden. *Int. J. Syst. Evol. Microbiol.* **1998**, *48*, 311–315. [CrossRef]
75. Sakaguchi, T.; Arakaki, A.; Matsunaga, T. *Desulfovibrio magneticus* sp. nov., a novel sulfate-reducing bacterium that produces intracellular single-domain-sized magnetite particles. *Int. J. Syst. Evol. Microbiol.* **2002**, *52*, 215–221. [CrossRef] [PubMed]
76. Legall, J. A New species of *Desulfovibrio*. *J. Bacteriol.* **1963**, *86*, 1120. [CrossRef] [PubMed]
77. Loubinoux, J.; Valente, F.M.A.; Pereira, I.A.C.; Costa, A.; Grimont, P.A.D.; Le Faou, A.E. Reclassification of the only species of the genus *Desulfomonas*, *Desulfomonas pigra*, as *Desulfovibrio piger* comb. nov. *Int. J. Syst. Evol. Microbiol.* **2002**, *52*, 1305–1308. [CrossRef] [PubMed]
78. Krekeler, D.; Sigalevich, P.; Teske, A.; Cypionka, H.; Cohen, Y. A sulfate-reducing bacterium from the oxic layer of a microbial mat from Solar Lake (Sinai), *Desulfovibrio oxyclinae* sp. nov. *Arch. Microbiol.* **1997**, *167*, 369–375. [CrossRef]
79. Sass, H.; Berchtold, M.; Branke, J.; König, H.; Cypionka, H.; Babenzien, H.-D. Psychrotolerant Sulfate-reducing Bacteria from an Oxic Freshwater Sediment Description of *Desulfovibrio cuneatus* sp. nov. and *Desulfovibrio litoralis* sp. nov. *Syst. Appl. Microbiol.* **1998**, *21*, 212–219. [CrossRef]
80. Klouche, N.; Basso, O.; Lascourrèges, J.-F.; Cayol, J.-L.; Thomas, P.; Fauque, G.; Fardeau, M.-L.; Magot, M. *Desulfocurvus vexinensis* gen. nov., sp. nov., a sulfate-reducing bacterium isolated from a deep subsurface aquifer. *Int. J. Syst. Evol. Microbiol.* **2009**, *59*, 3100–3104. [CrossRef]
81. Abildgaard, L.; Nielsen, M.B.; Kjeldsen, K.U.; Ingvorsen, K. *Desulfovibrio alkalitolerans* sp. nov., a novel alkalitolerant, sulphate-reducing bacterium isolated from district heating water. *Int. J. Syst. Evol. Microbiol.* **2006**, *56*, 1019–1024. [CrossRef]
82. Ollivier, B.; Cord-Ruwisch, R.; Hatchikian, E.C.; Garcia, J.L. Characterization of *Desulfovibrio fructosovorans* sp. nov. *Arch. Microbiol.* **1988**, *149*, 447–450. [CrossRef]
83. Alazard, D.; Dukan, S.; Urios, A.; Verhé, F.; Bouabida, N.; Morel, F.; Thomas, P.; Garcia, J.-L.; Ollivier, B. *Desulfovibrio hydrothermalis* sp. nov., a novel sulfate-reducing bacterium isolated from hydrothermal vents. *Int. J. Syst. Evol. Microbiol.* **2003**, *53*, 173–178. [CrossRef]
84. Brown, S.D.; Hurt, R.A., Jr.; Gilmour, C.C.; Elias, D.A. Draft genome sequences for three mercury-methylating, sulfate-reducing bacteria. *Genome Announc.* **2013**, *1*, e00618-13. [CrossRef] [PubMed]
85. Karnachuk, O.V.; Sasaki, K.; Gerasimchuk, A.L.; Sukhanova, O.; Ivasenko, D.A.; Kaksonen, A.H.; Puhakka, J.A.; Tuovinen, O.H. Precipitation of Cu-Sulfides by Copper-Tolerant *Desulfovibrio* Isolates. *Geomicrobiol. J.* **2008**, *25*, 219–227. [CrossRef]
86. Mancini, S.; Abicht, H.K.; Karnachuk, O.V.; Solioz, M. Genome sequence of *Desulfovibrio* sp. A2, a highly copper resistant, sulfate-reducing bacterium isolated from effluents of a zinc smelter at the Urals. *J. Bacteriol.* **2011**, *193*, 6793–6794. [CrossRef] [PubMed]
87. Baena, S.; Fardeau, M.L.; Labat, M.; Ollivier, B.; Garcia, J.L.; Patel, B.K. *Desulfovibrio aminophilus* sp. nov., a novel amino acid degrading and sulfate reducing bacterium from an anaerobic dairy wastewater lagoon. *Syst. Appl. Microbiol.* **1998**, *21*, 498–504. [CrossRef] [PubMed]
88. Khelaifia, S.; Fardeau, M.-L.; Pradel, N.; Aussignargues, C.; Garel, M.; Tamburini, C.; Cayol, J.-L.; Gaudron, S.; Gaill, F.; Ollivier, B. *Desulfovibrio piezophilus* sp. nov., a piezophilic, sulfate-reducing bacterium isolated from wood falls in the Mediterranean Sea. *Int. J. Syst. Evol. Microbiol.* **2011**, *61*, 2706–2711. [CrossRef]
89. Feio, M.J.; Zinkevich, V.; Beech, I.B.; Llobet-Brossa, E.; Eaton, P.; Schmitt, J.; Guezennec, J. *Desulfovibrio alaskensis* sp. nov., a sulphate-reducing bacterium from a soured oil reservoir. *Int. J. Syst. Evol. Microbiol.* **2004**, *54*, 1747–1752. [CrossRef]
90. Ramsay, B.D.; Hwang, C.; Woo, H.L.; Carroll, S.L.; Lucas, S.; Han, J.; Lapidus, A.L.; Cheng, J.F.; Goodwin, L.A.; Pitluck, S.; et al. High-Quality Draft Genome Sequence of *Desulfovibrio carbinoliphilus* FW-101-2B, an Organic Acid-Oxidizing Sulfate-Reducing Bacterium Isolated from Uranium(VI)-Contaminated Groundwater. *Genome Announc.* **2015**, *3*, e00092-15. [CrossRef]
91. Zhou, J.; He, Q.; Hemme, C.L.; Mukhopadhyay, A.; Hillesland, K.; Zhou, A.; He, Z.; Van Nostrand, J.D.; Hazen, T.C.; Stahl, D.A.; et al. How sulphate-reducing microorganisms cope with stress: Lessons from systems biology. *Nat. Rev. Microbiol.* **2011**, *9*, 452–466. [CrossRef]
92. Magot, M.; Basso, O.; Tardy-Jacquenod, C.; Caumette, P. *Desulfovibrio bastinii* sp. nov. and *Desulfovibrio gracilis* sp. nov., moderately halophilic, sulfate-reducing bacteria isolated from deep subsurface oilfield water. *Int. J. Syst. Evol. Microbiol.* **2004**, *54*, 1693–1697. [CrossRef]
93. Qatibi, A.-I.; Nivière, V.; Garcia, J. *Desulfovibrio alcoholovorans* sp. nov., a sulfate-reducing bacterium able to grow on glycerol, 1,2- and 1,3-propanediol. *Arch. Microbiol.* **1991**, *155*, 143–148. [CrossRef]
94. Nielsen, J.T.; Liesack, W.; Finster, K. *Desulfovibrio zosterae* sp. nov., a new sulfate reducer isolated from surface-sterilized roots of the seagrass *Zostera marina*. *Int. J. Syst. Evol. Microbiol.* **1999**, *49*, 859–865. [CrossRef]
95. Basso, O.; Caumette, P.; Magot, M. *Desulfovibrio putealis* sp. nov., a novel sulfate-reducing bacterium isolated from a deep subsurface aquifer. *Int. J. Syst. Evol. Microbiol.* **2005**, *55*, 101–104. [CrossRef] [PubMed]
96. Reichenbecher, W.; Schink, B. *Desulfovibrio inopinatus*, sp. nov., a new sulfate-reducing bacterium that degrades hydroxyhydroquinone (1,2,4-trihydroxybenzene). *Arch. Microbiol.* **1997**, *168*, 338–344. [CrossRef] [PubMed]

97. Magot, M.; Caumette, P.; Desperrier, J.M.; Matheron, R.; Dauga, C.; Grimont, F.; Carreau, L. *Desulfovibrio longus* sp. nov., a Sulfate-Reducing Bacterium Isolated from an Oil-Producing Well. *Int. J. Syst. Evol. Microbiol.* **1992**, *42*, 398–402. [CrossRef] [PubMed]
98. Gilmour, C.C.; Soren, A.B.; Gionfriddo, C.M.; Podar, M.; Wall, J.D.; Brown, S.D.; Michener, J.K.; Urriza, M.S.G.; Elias, D.A. *Pseudodesulfovibrio mercurii* sp. nov., a mercury-methylating bacterium isolated from sediment. *Int. J. Syst. Evol. Microbiol.* **2021**, *71*, 004697. [CrossRef]
99. Wolicka, D.; Jarzynowska, L. Microbiological Reduction of Sulphates in Salty Environments and Mineralogical Characterization of the Transformation Products. *Geomicrobiol. J.* **2012**, *29*, 528–536. [CrossRef]
100. Karnachuk, O.V.; Rusanov, I.I.; Panova, I.A.; Grigoriev, M.A.; Zyusman, V.S.; Latygolets, E.A.; Kadyrbaev, M.K.; Gruzdev, E.V.; Beletsky, A.V.; Mardanov, A.V.; et al. Microbial sulfate reduction by *Desulfovibrio* is an important source of hydrogen sulfide from a large swine finishing facility. *Sci. Rep.* **2021**, *11*, 10720. [CrossRef]
101. Boeckman, J.; Korn, A.; Yao, G.; Ravindran, A.; Gonzalez, C.; Gill, J. Sheep in wolves' clothing: Temperate T7-like bacteriophages and the origins of the *Autographiviridae*. *Virology* **2022**, *568*, 86–100. [CrossRef]
102. Hatchikian, E.C.; Forget, N.; Fernandez, V.M.; Williams, R.; Cammack, R. Further characterization of the [Fe]-hydrogenase from *Desulfovibrio desulfuricans* ATCC 7757. *Eur. J. Biochem.* **1992**, *209*, 357–365. [CrossRef]
103. Day, L.A.; León, K.B.D.; Kempher, M.L.; Zhou, J.; Wall, J.D. Complete Genome Sequence of *Desulfovibrio desulfuricans* IC1, a Sulfonate-Respiring Anaerobe. *Microbiol. Resour. Announc.* **2019**, *8*, 10–1128. [CrossRef]
104. Lie, T.J.; Pitta, T.; Leadbetter, E.R.; Godchaux Iii, W.; Leadbetter, J.R. Sulfonates: Novel electron acceptors in anaerobic respiration. *Arch. Microbiol.* **1996**, *166*, 204–210. [CrossRef]
105. Sheik, C.S.; Sieber, J.R.; Badalamenti, J.P.; Carden, K.; Olson, A. Complete Genome Sequence of *Desulfovibrio desulfuricans* Strain G11, a Model Sulfate-Reducing, Hydrogenotrophic, and Syntrophic Partner Organism. *Genome Announc.* **2017**, *5*, 10–1128. [CrossRef] [PubMed]
106. McInerney, M.J.; Bryant, M.P.; Pfennig, N. Anaerobic bacterium that degrades fatty acids in syntrophic association with methanogens. *Arch. Microbiol.* **1979**, *122*, 129–135. [CrossRef]
107. Karnachuk, O.V.; Ikkert, O.P.; Avakyan, M.R.; Knyazev, Y.V.; Volochaev, N.M.; Zyusman, V.S.; Panov, V.L.; Kadnikov, V.V.; Mardanov, A.V.; Ravin, N.V. *Desulfovibrio desulfuricans* AY5 Isolated from a Patient with Autism Spectrum Disorder Binds Iron in Low-Soluble Greigite and Pyrite. *Microorganisms* **2021**, *9*, 2558. [CrossRef]
108. Sun, D.; Wang, A.; Cheng, S.; Yates, M.; Logan, B.E. *Geobacter anodireducens* sp. nov., an exoelectrogenic microbe in bioelectrochemical systems. *Int. J. Syst. Evol. Microbiol.* **2014**, *64*, 3485–3491. [CrossRef]
109. Shelobolina, E.S.; Nevin, K.P.; Blakeney-Hayward, J.D.; Johnsen, C.V.; Plaia, T.W.; Krader, P.; Woodard, T.; Holmes, D.E.; VanPraagh, C.G.; Lovley, D.R. *Geobacter pickeringii* sp. nov., *Geobacter argillaceus* sp. nov. and *Pelosinus fermentans* gen. nov., sp. nov., isolated from subsurface kaolin lenses. *Int. J. Syst. Evol. Microbiol.* **2007**, *57*, 126–135. [CrossRef] [PubMed]
110. Coates, J.D.; Bhupathiraju, V.K.; Achenbach, L.A.; Mclnerney, M.J.; Lovley, D.R. *Geobacter hydrogenophilus*, *Geobacter chapellei* and *Geobacter grbiciae*, three new, strictly anaerobic, dissimilatory Fe(III)-reducers. *Int. J. Syst. Evol. Microbiol.* **2001**, *51*, 581–588. [CrossRef]
111. Prakash, O.; Gihring, T.M.; Dalton, D.D.; Chin, K.-J.; Green, S.J.; Akob, D.M.; Wanger, G.; Kostka, J.E. *Geobacter daltonii* sp. nov., an Fe(III)- and uranium(VI)-reducing bacterium isolated from a shallow subsurface exposed to mixed heavy metal and hydrocarbon contamination. *Int. J. Syst. Evol. Microbiol.* **2010**, *60*, 546–553. [CrossRef] [PubMed]
112. Viulu, S.; Nakamura, K.; Okada, Y.; Saitou, S.; Takamizawa, K. *Geobacter luticola* sp. nov., an Fe(III)-reducing bacterium isolated from lotus field mud. *Int. J. Syst. Evol. Microbiol.* **2013**, *63*, 442–448. [CrossRef]
113. Childers, S.E.; Ciufo, S.; Lovley, D.R. *Geobacter metallireducens* accesses insoluble Fe(III) oxide by chemotaxis. *Nature* **2002**, *416*, 767–769. [CrossRef]
114. Aklujkar, M.; Krushkal, J.; DiBartolo, G.; Lapidus, A.; Land, M.L.; Lovley, D.R. The genome sequence of *Geobacter metallireducens*: Features of metabolism, physiology and regulation common and dissimilar to *Geobacter sulfurreducens*. *BMC Microbiol.* **2009**, *9*, 109. [CrossRef] [PubMed]
115. Lovley, D.R.; Phillips, E.J. Novel mode of microbial energy metabolism: Organic carbon oxidation coupled to dissimilatory reduction of iron or manganese. *Appl. Environ. Microbiol.* **1988**, *54*, 1472–1480. [CrossRef] [PubMed]
116. Badalamenti, J.P.; Bond, D.R. Complete Genome of *Geobacter pickeringii* G13 T, a Metal-Reducing Isolate from Sedimentary Kaolin Deposits. *Genome Announc.* **2015**, *3*, e00038-15. [CrossRef]
117. Yang, G.; Chen, S.; Zhou, S.; Liu, Y. Genome sequence of a dissimilatory Fe(III)-reducing bacterium *Geobacter soli* type strain GSS01(T). *Stand Genom. Sci.* **2015**, *10*, 118. [CrossRef]
118. Guo, Y.; Aoyagi, T.; Hori, T. Draft Genome Sequences of the Ferric Iron-Reducing *Geobacter* sp. Strains AOG1 and AOG2, Isolated from Enrichment Cultures on Crystalline Iron(III) Oxides. *Microbiol. Resour. Announc.* **2021**, *10*, e0091321. [CrossRef]
119. Hori, T.; Aoyagi, T.; Itoh, H.; Narihiro, T.; Oikawa, A.; Suzuki, K.; Ogata, A.; Friedrich, M.W.; Conrad, R.; Kamagata, Y. Isolation of microorganisms involved in reduction of crystalline iron(III) oxides in natural environments. *Front. Microbiol.* **2015**, *6*, 386. [CrossRef]
120. Yadav, P.; Antony-Babu, S.; Hayes, E.; Healy, O.M.; Pan, D.; Yang, W.H.; Silver, W.L.; Anderson, C.L.; Voshall, A.; Fernando, S.C.; et al. Complete Genome Sequence of *Geobacter* sp. Strain FeAm09, a Moderately Acidophilic Soil Bacterium. *Microbiol. Resour. Announc.* **2021**, *10*, 10–1128. [CrossRef] [PubMed]

121. Yang, G.; Li, Y.; Lin, A.; Zhuang, L. *Geobacter benzoatilyticus* sp. nov., a novel benzoate-oxidizing, iron-reducing bacterium isolated from petroleum contaminated soil. *Int. J. Syst. Evol. Microbiol.* **2022**, *72*, 005281. [CrossRef]
122. Ehara, A.; Suzuki, H.; Amachi, S. Draft Genome Sequence of *Geobacter sp.* Strain OR-1, an Arsenate-Respiring Bacterium Isolated from Japanese Paddy Soil. *Genome Announc.* **2015**, *3*, e01478-14. [CrossRef]
123. Ohtsuka, T.; Yamaguchi, N.; Makino, T.; Sakurai, K.; Kimura, K.; Kudo, K.; Homma, E.; Dong, D.T.; Amachi, S. Arsenic Dissolution from Japanese Paddy Soil by a Dissimilatory Arsenate-Reducing Bacterium *Geobacter* sp. OR-1. *Environ. Sci. Technol.* **2013**, *47*, 6263–6271. [CrossRef]
124. Warashina, T.; Yamamura, S.; Suzuki, H.; Amachi, S.; Arakawa, K. Complete Genome Sequence of *Geobacter* sp. Strain SVR, an Antimonate-Reducing Bacterium Isolated from Antimony-Rich Mine Soil. *Microbiol. Resour. Announc.* **2021**, *10*, 10–1128. [CrossRef]
125. Warashina, T.; Harada, M.; Nakajima, N.; Yamamura, S.; Tomita, M.; Suzuki, H.; Amachi, S. Draft Genome Sequence of *Geobacter* sp. Strain SVR, Isolated from Antimony Mine Soil. *Microbiol. Resour. Announc.* **2020**, *9*, 10-1128. [CrossRef] [PubMed]
126. Yamamura, S.; Iida, C.; Kobayashi, Y.; Watanabe, M.; Amachi, S. Production of two morphologically different antimony trioxides by a novel antimonate-reducing bacterium, *Geobacter* sp. SVR. *J. Hazard. Mater.* **2021**, *411*, 125100. [CrossRef] [PubMed]
127. Nagarajan, H.; Butler, J.E.; Klimes, A.; Qiu, Y.; Zengler, K.; Ward, J.; Young, N.D.; Methé, B.A.; Palsson, B.; Lovley, D.R.; et al. *De Novo* assembly of the complete genome of an enhanced electricity-producing variant of *Geobacter sulfurreducens* using only short reads. *PLoS ONE* **2010**, *5*, e10922. [CrossRef]
128. Yi, H.; Nevin, K.P.; Kim, B.C.; Franks, A.E.; Klimes, A.; Tender, L.M.; Lovley, D.R. Selection of a variant of *Geobacter sulfurreducens* with enhanced capacity for current production in microbial fuel cells. *Biosens. Bioelectron.* **2009**, *24*, 3498–3503. [CrossRef]
129. Caccavo, F., Jr.; Lonergan, D.J.; Lovley, D.R.; Davis, M.; Stolz, J.F.; McInerney, M.J. *Geobacter sulfurreducens* sp. nov., a hydrogen- and acetate-oxidizing dissimilatory metal-reducing microorganism. *Appl. Environ. Microbiol.* **1994**, *60*, 3752–3759. [CrossRef]
130. Methé, B.A.; Nelson, K.E.; Eisen, J.A.; Paulsen, I.T.; Nelson, W.; Heidelberg, J.F.; Wu, D.; Wu, M.; Ward, N.; Beanan, M.J.; et al. Genome of *Geobacter sulfurreducens*: Metal reduction in subsurface environments. *Science* **2003**, *302*, 1967–1969. [CrossRef] [PubMed]
131. Inoue, K.; Ogura, Y.; Kawano, Y.; Hayashi, T. Complete Genome Sequence of *Geobacter sulfurreducens* Strain YM18, Isolated from River Sediment in Japan. *Genome Announc.* **2018**, *6*, e00352-18. [CrossRef]
132. Fujikawa, T.; Ogura, Y.; Ishigami, K.; Kawano, Y.; Nagamine, M.; Hayashi, T.; Inoue, K. Unexpected genomic features of high current density-producing *Geobacter sulfurreducens* strain YM18. *FEMS Microbiol. Lett.* **2021**, *368*, fnab119. [CrossRef]
133. Fujikawa, T.; Ogura, Y.; Hayashi, T.; Inoue, K. Complete Genome Sequence of High Current-Producing *Geobacter sulfurreducens* Strain YM35, Isolated from River Sediment in Japan. *Microbiol. Resour. Announc.* **2021**, *10*, e0053921. [CrossRef]
134. Shelobolina, E.S.; Vrionis, H.A.; Findlay, R.H.; Lovley, D.R. *Geobacter uraniireducens* sp. nov., isolated from subsurface sediment undergoing uranium bioremediation. *Int. J. Syst. Evol. Microbiol.* **2008**, *58*, 1075–1078. [CrossRef] [PubMed]
135. Semple, K.M.; Westlake, D.W.S. Characterization of iron-reducing *Alteromonas putrefaciens* strains from oil field fluids. *Can. J. Microbiol.* **1987**, *33*, 366–371. [CrossRef]
136. Kim, J.-Y.; Yoo, H.-S.; Lee, D.-H.; Park, S.-H.; Kim, Y.-J.; Oh, D.-C. *Shewanella algicola* sp. nov., a marine bacterium isolated from brown algae. *Int. J. Syst. Evol. Microbiol.* **2016**, *66*, 2218–2224. [CrossRef] [PubMed]
137. Ohama, Y.; Aoki, K.; Harada, S.; Nagasawa, T.; Sawabe, T.; Nonaka, L.; Moriya, K.; Ishii, Y.; Tateda, K. Genetic Environment Surrounding $bla_{OXA-55-like}$ in Clinical Isolates of *Shewanella algae* Clade and Enhanced Expression of $bla_{OXA-55-like}$ in a Carbapenem-Resistant Isolate. *mSphere* **2021**, *6*, e00593-21. [CrossRef]
138. Wang, Y.; Chen, H.; Liu, Z.; Ming, H.; Zhou, C.; Zhu, X.; Zhang, P.; Jing, C.; Feng, H. *Shewanella gelidii* sp. nov., isolated from the red algae *Gelidium amansii*, and emended description of *Shewanella waksmanii*. *Int. J. Syst. Evol. Microbiol.* **2016**, *66*, 2899–2905. [CrossRef] [PubMed]
139. Satomi, M.; Vogel, B.F.; Venkateswaran, K.; Gram, L. Description of *Shewanella glacialipiscicola* sp. nov. and *Shewanella algidipiscicola* sp. nov., isolated from marine fish of the Danish Baltic Sea, and proposal that Shewanella affinis is a later heterotypic synonym of *Shewanella colwelliana*. *Int. J. Syst. Evol. Microbiol.* **2007**, *57*, 347–352. [CrossRef]
140. Satomi, M.; Vogel, B.F.; Gram, L.; Venkateswaran, K. *Shewanella hafniensis* sp. nov. and *Shewanella morhuae* sp. nov., isolated from marine fish of the Baltic Sea. *Int. J. Syst. Evol. Microbiol.* **2006**, *56*, 243–249. [CrossRef] [PubMed]
141. Prachumwat, A.; Wechprasit, P.; Srisala, J.; Kriangsaksri, R.; Flegel, T.W.; Thitamadee, S.; Sritunyalucksana, K. *Shewanella khirikhana* sp. nov.—A shrimp pathogen isolated from a cultivation pond exhibiting early mortality syndrome. *Microb. Biotechnol.* **2020**, *13*, 781–795. [CrossRef] [PubMed]
142. Wechprasit, P.; Panphloi, M.; Thitamadee, S.; Sritunyalucksana, K.; Prachumwat, A. Complete Genome Sequence of *Shewanella* sp. Strain TH2012, Isolated from Shrimp in a Cultivation Pond Exhibiting Early Mortality Syndrome. *Microbiol. Resour. Announc.* **2019**, *8*, e01703-18. [CrossRef]
143. Leonardo, M.R.; Moser, D.P.; Barbieri, E.; Brantner, C.A.; MacGregor, B.J.; Paster, B.J.; Stackebrandt, E.; Nealson, K.H. *Shewanella pealeana* sp. nov., a member of the microbial community associated with the accessory nidamental gland of the squid *Loligo pealei*. *Int. J. Syst. Bacteriol.* **1999**, *49 Pt 4*, 1341–1351. [CrossRef]
144. Cha, Q.-Q.; Ren, X.-B.; Sun, Y.-Y.; He, X.-Y.; Su, H.-N.; Chen, X.-L.; Zhang, Y.-Z.; Xie, B.-B.; Zhao, L.-S.; Song, X.-Y.; et al. *Shewanella polaris* sp. nov., a psychrotolerant bacterium isolated from Arctic brown algae. *Int. J. Syst. Evol. Microbiol.* **2020**, *70*, 2096–2102. [CrossRef] [PubMed]

145. Gai, Y.; Huang, Z.; Lai, Q.; Shao, Z. *Shewanella intestini* sp. nov., isolated from the intestine of abalone, *Haliotis diversicolor*. *Int. J. Syst. Evol. Microbiol.* **2017**, *67*, 1901–1905. [CrossRef] [PubMed]
146. Satomi, M.; Oikawa, H.; Yano, Y. *Shewanella marinintestina* sp. nov., *Shewanella schlegeliana* sp. nov. and *Shewanella sairae* sp. nov., novel eicosapentaenoic-acid-producing marine bacteria isolated from sea-animal intestines. *Int. J. Syst. Evol. Microbiol.* **2003**, *53*, 491–499. [CrossRef] [PubMed]
147. Brian-Jaisson, F.; Ortalo-Magné, A.; Guentas-Dombrowsky, L.; Armougom, F.; Blache, Y.; Molmeret, M. Identification of bacterial strains isolated from the Mediterranean Sea exhibiting different abilities of biofilm formation. *Microb. Ecol.* **2014**, *68*, 94–110. [CrossRef]
148. Guillonneau, R.; Baraquet, C.; Bazire, A.; Molmeret, M. Multispecies Biofilm Development of Marine Bacteria Implies Complex Relationships Through Competition and Synergy and Modification of Matrix Components. *Front. Microbiol.* **2018**, *9*, 1960. [CrossRef]
149. Caro-Quintero, A.; Auchtung, J.; Deng, J.; Brettar, I.; Höfle, M.; Tiedje, J.M.; Konstantinidis, K.T. Genome sequencing of five *Shewanella baltica* strains recovered from the oxic-anoxic interface of the Baltic Sea. *J. Bacteriol.* **2012**, *194*, 1236. [CrossRef]
150. Deng, J.; Brettar, I.; Luo, C.; Auchtung, J.; Konstantinidis, K.T.; Rodrigues, J.L.; Höfle, M.; Tiedje, J.M. Stability, genotypic and phenotypic diversity of *Shewanella baltica* in the redox transition zone of the Baltic Sea. *Environ. Microbiol.* **2014**, *16*, 1854–1866. [CrossRef]
151. Sung, H.-R.; Yoon, J.-H.; Ghim, S.-Y. *Shewanella dokdonensis* sp. nov., isolated from seawater. *Int. J. Syst. Evol. Microbiol.* **2012**, *62*, 1636–1643. [CrossRef] [PubMed]
152. Reid, G.A.; Gordon, E.H.J. Phylogeny of marine and freshwater *Shewanella*: Reclassification of *Shewanella putrefaciens* NCIMB 400 as *Shewanella frigidimarina*. *Int. J. Syst. Evol. Microbiol.* **1999**, *49*, 189–191. [CrossRef]
153. Reyes-Ramirez, F.; Dobbin, P.; Sawers, G.; Richardson David, J. Characterization of Transcriptional Regulation of *Shewanella frigidimarina* Fe(III)-Induced Flavocytochrome c Reveals a Novel Iron-Responsive Gene Regulation System. *J. Bacteriol.* **2003**, *185*, 4564–4571. [CrossRef]
154. Kim, K.M.; Choe, H.; Kim, B.K.; Nasir, A. Complete genome of a metabolically-diverse marine bacterium *Shewanella japonica* KCTC 22435(T). *Mar. Genom.* **2017**, *35*, 39–42. [CrossRef]
155. Biffinger, J.C.; Fitzgerald, L.A.; Ray, R.; Little, B.J.; Lizewski, S.E.; Petersen, E.R.; Ringeisen, B.R.; Sanders, W.C.; Sheehan, P.E.; Pietron, J.J.; et al. The utility of *Shewanella japonica* for microbial fuel cells. *Bioresour. Technol.* **2011**, *102*, 290–297. [CrossRef]
156. Ivanova, E.P.; Sawabe, T.; Gorshkova, N.M.; Svetashev, V.I.; Mikhailov, V.V.; Nicolau, D.V.; Christen, R. *Shewanella japonica* sp. nov. *Int. J. Syst. Evol. Microbiol.* **2001**, *51*, 1027–1033. [CrossRef]
157. Yun, B.-R.; Park, S.; Kim, M.-K.; Park, J.; Kim, S.B. Shewanella saliphila sp. nov., Shewanella ulleungensis sp. nov. and Shewanella litoralis sp. nov., isolated from coastal seawater. *Int. J. Syst. Evol. Microbiol.* **2018**, *68*, 2960–2966. [CrossRef] [PubMed]
158. Bozal, N.; Montes, M.J.; Tudela, E.; Jiménez, F.; Guinea, J. *Shewanella frigidimarina* and *Shewanella livingstonensis* sp. nov. isolated from Antarctic coastal areas. *Int. J. Syst. Evol. Microbiol.* **2002**, *52*, 195–205. [CrossRef] [PubMed]
159. Park, S.C.; Baik, K.S.; Kim, M.S.; Kim, D.; Seong, C.N. *Shewanella marina* sp. nov., isolated from seawater. *Int. J. Syst. Evol. Microbiol.* **2009**, *59*, 1888–1894. [CrossRef] [PubMed]
160. Bae, S.S.; Jung, Y.-h.; Baek, K. *Shewanella maritima* sp. nov., a facultative anaerobic marine bacterium isolated from seawater, and emended description of *Shewanella intestini*. *Int. J. Syst. Evol. Microbiol.* **2020**, *70*, 1288–1293. [CrossRef]
161. Makemson, J.C.; Fulayfil, N.R.; Landry, W.; Van Ert, L.M.; Wimpee, C.F.; Widder, E.A.; Case, J.F. *Shewanella woodyi* sp. nov., an exclusively respiratory luminous bacterium isolated from the Alboran Sea. *Int. J. Syst. Bacteriol.* **1997**, *47*, 1034–1039. [CrossRef]
162. Park, H.Y.; Jeon, C.O. *Shewanella aestuarii* sp. nov., a marine bacterium isolated from a tidal flat. *Int. J. Syst. Evol. Microbiol.* **2013**, *63*, 4683–4690. [CrossRef]
163. Baaziz, H.; Lemaire, O.N.; Jourlin-Castelli, C.; Iobbi-Nivol, C.; Méjean, V.; Alatou, R.; Fons, M. Draft Genome Sequence of *Shewanella algidipiscicola* H1, a Highly Chromate-Resistant Strain Isolated from Mediterranean Marine Sediments. *Microbiol. Resour. Announc.* **2018**, *7*, e00905-18. [CrossRef]
164. Venkateswaran, K.; Dollhopf, M.E.; Aller, R.; Stackebrandt, E.; Nealson, K.H. *Shewanella amazonensis* sp. nov., a novel metal-reducing facultative anaerobe from Amazonian shelf muds. *Int. J. Syst. Bacteriol.* **1998**, *48 Pt 3*, 965–972. [CrossRef] [PubMed]
165. Sucharita, K.; Sasikala, C.; Park, S.C.; Baik, K.S.; Seong, C.N.; Ramana, C.V. *Shewanella chilikensis* sp. nov., a moderately alkaliphilic gammaproteobacterium isolated from a lagoon. *Int. J. Syst. Evol. Microbiol.* **2009**, *59*, 3111–3115. [CrossRef]
166. Yang, S.-H.; Lee, J.-H.; Ryu, J.-S.; Kato, C.; Kim, S.-J. *Shewanella donghaensis* sp. nov., a psychrophilic, piezosensitive bacterium producing high levels of polyunsaturated fatty acid, isolated from deep-sea sediments. *Int. J. Syst. Evol. Microbiol.* **2007**, *57*, 208–212. [CrossRef]
167. Ivanova, E.P.; Sawabe, T.; Hayashi, K.; Gorshkova, N.M.; Zhukova, N.V.; Nedashkovskaya, O.I.; Mikhailov, V.V.; Nicolau, D.V.; Christen, R. *Shewanella fidelis* sp. nov., isolated from sediments and sea water. *Int. J. Syst. Evol. Microbiol.* **2003**, *53*, 577–582. [CrossRef] [PubMed]
168. Verma, P.; Pandey, P.K.; Gupta, A.K.; Kim, H.J.; Baik, K.S.; Seong, C.N.; Patole, M.S.; Shouche, Y.S. *Shewanella indica* sp. nov., isolated from sediment of the Arabian Sea. *Int. J. Syst. Evol. Microbiol.* **2011**, *61*, 2058–2064. [CrossRef]
169. Wang, M.-q.; Sun, L. *Shewanella inventionis* sp. nov., isolated from deep-sea sediment. *Int. J. Syst. Evol. Microbiol.* **2016**, *66*, 4947–4953. [CrossRef]

170. Lee, M.H.; Yoon, J.H. *Shewanella litorisediminis* sp. nov., a gammaproteobacterium isolated from a tidal flat sediment. *Antonie Van Leeuwenhoek* **2012**, *102*, 591–599. [CrossRef]
171. Liu, Y.; Shang, X.-X.; Yi, Z.-W.; Gu, L.; Zeng, R.-Y. *Shewanella mangrovi* sp. nov., an acetaldehyde-degrading bacterium isolated from mangrove sediment. *Int. J. Syst. Evol. Microbiol.* **2015**, *65*, 2630–2634. [CrossRef] [PubMed]
172. Huang, J.; Sun, B.; Zhang, X. Electricity generation at high ionic strength in microbial fuel cell by a newly isolated *Shewanella marisflavi* EP1. *Appl. Microbiol. Biotechnol.* **2010**, *85*, 1141–1149. [CrossRef]
173. Huang, J.; Ning, G.; Li, F.; Sheng, G.D. Biotransformation of 2,4-dinitrotoluene by obligate marine *Shewanella marisflavi* EP1 under anaerobic conditions. *Bioresour. Technol.* **2015**, *180*, 200–206. [CrossRef]
174. Venkateswaran, K.; Moser, D.P.; Dollhopf, M.E.; Lies, D.P.; Saffarini, D.A.; MacGregor, B.J.; Ringelberg, D.B.; White, D.C.; Nishijima, M.; Sano, H.; et al. Polyphasic taxonomy of the genus *Shewanella* and description of *Shewanella oneidensis* sp. nov. *Int. J. Syst. Evol. Microbiol.* **1999**, *49*, 705–724. [CrossRef] [PubMed]
175. Heidelberg, J.F.; Paulsen, I.T.; Nelson, K.E.; Gaidos, E.J.; Nelson, W.C.; Read, T.D.; Eisen, J.A.; Seshadri, R.; Ward, N.; Methe, B.; et al. Genome sequence of the dissimilatory metal ion–reducing bacterium *Shewanella oneidensis*. *Nat. Biotechnol.* **2002**, *20*, 1118–1123. [CrossRef] [PubMed]
176. Xiao, X.; Wang, P.; Zeng, X.; Bartlett, D.H.; Wang, F. *Shewanella psychrophila* sp. nov. and *Shewanella piezotolerans* sp. nov., isolated from west Pacific deep-sea sediment. *Int. J. Syst. Evol. Microbiol.* **2007**, *57*, 60–65. [CrossRef] [PubMed]
177. Wang, F.; Wang, J.; Jian, H.; Zhang, B.; Li, S.; Wang, F.; Zeng, X.; Gao, L.; Bartlett, D.H.; Yu, J.; et al. Environmental adaptation: Genomic analysis of the piezotolerant and psychrotolerant deep-sea iron reducing bacterium *Shewanella piezotolerans* WP3. *PLoS ONE* **2008**, *3*, e1937. [CrossRef]
178. Xu, G.; Jian, H.; Xiao, X.; Wang, F. Complete genome sequence of *Shewanella psychrophila* WP2, a deep-sea bacterium isolated from west Pacific sediment. *Mar. Genom.* **2017**, *35*, 19–21. [CrossRef]
179. Li, S.; Niu, Y.; Chen, H.; He, P. Complete genome sequence of an Arctic Ocean bacterium *Shewanella* sp. Arc9-LZ with capacity of synthesizing silver nanoparticles in darkness. *Mar. Genom.* **2021**, *56*, 100808. [CrossRef]
180. Bujak, K.; Decewicz, P.; Rosinska, J.M.; Radlinska, M. Genome Study of a Novel Virulent Phage vB_SspS_KASIA and Mu-like Prophages of *Shewanella* sp. M16 Provides Insights into the Genetic Diversity of the *Shewanella* Virome. *Int. J. Mol. Sci.* **2021**, *22*, 11070. [CrossRef]
181. Yang, Y.; Chen, J.; Qiu, D.; Zhou, J. Roles of UndA and MtrC of *Shewanella putrefaciens* W3-18-1 in iron reduction. *BMC Microbiol.* **2013**, *13*, 267. [CrossRef] [PubMed]
182. Qiu, D.; Wei, H.; Tu, Q.; Yang, Y.; Xie, M.; Chen, J.; Pinkerton, M.H.; Liang, Y.; He, Z.; Zhou, J. Combined Genomics and Experimental Analyses of Respiratory Characteristics of *Shewanella putrefaciens* W3-18-1. *Appl. Environ. Microbiol.* **2013**, *79*, 5250–5257. [CrossRef]
183. Bozal, N.; Montes, M.J.; Miñana-Galbis, D.; Manresa, A.; Mercadé, E. *Shewanella vesiculosa* sp. nov., a psychrotolerant bacterium isolated from an Antarctic coastal area. *Int. J. Syst. Evol. Microbiol.* **2009**, *59*, 336–340. [CrossRef]
184. Nogi, Y.; Kato, C.; Horikoshi, K. Taxonomic studies of deep-sea barophilic *Shewanella* strains and description of *Shewanella violacea* sp. nov. *Arch. Microbiol.* **1998**, *170*, 331–338. [CrossRef]
185. Chikuma, S.; Kasahara, R.; Kato, C.; Tamegai, H. Bacterial adaptation to high pressure: A respiratory system in the deep-sea bacterium *Shewanella violacea* DSS12. *FEMS Microbiol. Lett.* **2007**, *267*, 108–112. [CrossRef] [PubMed]
186. Jensen, M.J.; Tebo, B.M.; Baumann, P.; Mandel, M.; Nealson, K.H. Characterization of *Alteromonas hanedai* (sp. nov.), a nonfermentative luminous species of marine origin. *Curr. Microbiol.* **1980**, *3*, 311–315. [CrossRef]
187. Lee, J.-H.; Roh, Y.; Kim, K.-W.; Hur, H.-G. Organic Acid-Dependent Iron Mineral Formation by a Newly Isolated Iron-Reducing Bacterium, *Shewanella* sp. HN-41. *Geomicrobiol. J.* **2007**, *24*, 31–41. [CrossRef]
188. Lee, J.H.; Kim, M.G.; Yoo, B.; Myung, N.V.; Maeng, J.; Lee, T.; Dohnalkova, A.C.; Fredrickson, J.K.; Sadowsky, M.J.; Hur, H.G. Biogenic formation of photoactive arsenic-sulfide nanotubes by *Shewanella* sp. strain HN-41. *Proc. Natl. Acad. Sci. USA* **2007**, *104*, 20410–20415. [CrossRef] [PubMed]
189. Zhao, J.-S.; Manno, D.; Leggiadro, C.; Leggiadro, C.; O'Neil, C.; O'Neil, C.; Hawari, J. *Shewanella halifaxensis* sp. nov., a novel obligately respiratory and denitrifying psychrophile. *Int. J. Syst. Evol. Microbiol.* **2006**, *56*, 205–212. [CrossRef]
190. Li, Z.; Song, F.; Chen, M. Complete Genome Sequence of *Shewanella* sp. Strain Lzh-2, an Algicidal Bacterial Strain Isolated from Lake Taihu, People's Republic of China. *Microbiol. Resour. Announc.* **2021**, *10*, e00339-21. [CrossRef]
191. Li, Z.; Lin, S.; Liu, X.; Tan, J.; Pan, J.; Yang, H. A freshwater bacterial strain, *Shewanella* sp. Lzh-2, isolated from Lake Taihu and its two algicidal active substances, hexahydropyrrolo[1,2-a]pyrazine-1,4-dione and 2, 3-indolinedione. *Appl. Microbiol. Biotechnol.* **2014**, *98*, 4737–4748. [CrossRef]
192. Boles, B.W.; Murdoch, R.W.; Ohlsson, I.; Mikucki, J.A. Draft Genome Sequence of *Shewanella* sp. Strain BF02_Schw, Isolated from Blood Falls, a Feature Where Subglacial Brine Discharges to the Surface of Taylor Glacier, Antarctica. *Microbiol. Resour. Announc.* **2021**, *10*, e01141-20. [CrossRef]
193. Sravan Kumar, R.; Sasi Jyothsna, T.S.; Sasikala, C.; Seong, C.N.; Lim, C.H.; Park, S.C.; Ramana, C.V. *Shewanella fodinae* sp. nov., isolated from a coal mine and from a marine lagoon. *Int. J. Syst. Evol. Microbiol.* **2010**, *60*, 1649–1654. [CrossRef]
194. Saltikov, C.W.; Cifuentes, A.; Venkateswaran, K.; Newman, D.K. The ars detoxification system is advantageous but not required for As(V) respiration by the genetically tractable *Shewanella species* strain ANA-3. *Appl. Environ. Microbiol.* **2003**, *69*, 2800–2809. [CrossRef] [PubMed]

195. Saltikov, C.W.; Wildman, R.A., Jr.; Newman, D.K. Expression dynamics of arsenic respiration and detoxification in *Shewanella* sp. strain ANA-3. *J. Bacteriol.* **2005**, *187*, 7390–7396. [CrossRef]
196. Zargar, K.; Saltikov, C.W. Lysine-91 of the tetraheme c-type cytochrome CymA is essential for quinone interaction and arsenate respiration in *Shewanella* sp. strain ANA-3. *Arch. Microbiol.* **2009**, *191*, 797–806. [CrossRef] [PubMed]
197. Qasim, M.S.; Lampi, M.; Heinonen, M.-M.K.; Garrido-Zabala, B.; Bamford, D.H.; Käkelä, R.; Roine, E.; Sarin, L.P. Cold-Active *Shewanella glacialimarina* TZS-4T nov. Features a Temperature-Dependent Fatty Acid Profile and Putative Sialic Acid Metabolism. *Front. Microbiol.* **2021**, *12*, 737641. [CrossRef]
198. Cao, W.-R.; Li, X.; Sun, Y.-Y.; Jiang, M.-Y.; Xu, X.-D.; Li, Y.-J. *Shewanella nanhaiensis* sp. nov., a marine bacterium isolated from sediment of South China Sea, and emended descriptions of *Shewanella woodyi*, *Shewanella hanedai* and *Shewanella canadensis*. *Int. J. Syst. Evol. Microbiol.* **2021**, *71*, 005152. [CrossRef]
199. Yu, N.Y.; Wagner, J.R.; Laird, M.R.; Melli, G.; Rey, S.; Lo, R.; Dao, P.; Sahinalp, S.C.; Ester, M.; Foster, L.J.; et al. PSORTb 3.0: Improved protein subcellular localization prediction with refined localization subcategories and predictive capabilities for all prokaryotes. *Bioinformatics* **2010**, *26*, 1608–1615. [CrossRef]
200. Ishii, S.I.; Suzuki, S.; Norden-Krichmar, T.M.; Tenney, A.; Chain, P.S.G.; Scholz, M.B.; Nealson, K.H.; Bretschger, O. A novel metatranscriptomic approach to identify gene expression dynamics during extracellular electron transfer. *Nat. Commun.* **2013**, *4*, 1601. [CrossRef] [PubMed]
201. Arndt, D.; Grant, J.R.; Marcu, A.; Sajed, T.; Pon, A.; Liang, Y.; Wishart, D.S. PHASTER: A better, faster version of the PHAST phage search tool. *Nucleic Acids Res.* **2016**, *44*, W16–W21. [CrossRef]
202. Makarova, K.S.; Wolf, Y.I.; Iranzo, J.; Shmakov, S.A.; Alkhnbashi, O.S.; Brouns, S.J.J.; Charpentier, E.; Cheng, D.; Haft, D.H.; Horvath, P.; et al. Evolutionary classification of CRISPR–Cas systems: A burst of class 2 and derived variants. *Nat. Rev. Microbiol.* **2020**, *18*, 67–83. [CrossRef] [PubMed]
203. Siguier, P.; Perochon, J.; Lestrade, L.; Mahillon, J.; Chandler, M. ISfinder: The reference centre for bacterial insertion sequences. *Nucleic Acids Res.* **2006**, *34*, D32–D36. [CrossRef]
204. Néron, B.; Littner, E.; Haudiquet, M.; Perrin, A.; Cury, J.; Rocha, E.P.C. IntegronFinder 2.0: Identification and Analysis of Integrons across Bacteria, with a Focus on Antibiotic Resistance in *Klebsiella*. *Microorganisms* **2022**, *10*, 700. [CrossRef] [PubMed]
205. Abby, S.S.; Néron, B.; Ménager, H.; Touchon, M.; Rocha, E.P.C. MacSyFinder: A Program to Mine Genomes for Molecular Systems with an Application to CRISPR-Cas Systems. *PLoS ONE* **2014**, *9*, e110726. [CrossRef] [PubMed]
206. Cury, J.; Touchon, M.; Rocha, E.P.C. Integrative and conjugative elements and their hosts: Composition, distribution and organization. *Nucleic Acids Res.* **2017**, *45*, 8943–8956. [CrossRef] [PubMed]
207. Bastian, M.; Heymann, S.; Jacomy, M. Gephi: An Open Source Software for Exploring and Manipulating Networks. In Proceedings of the International AAAI Conference on Web and Social Media, San Jose, CA, USA, 17–20 May 2009; Volume 3, pp. 361–362. [CrossRef]
208. Fruchterman, T.M.J.; Reingold, E.M. Graph drawing by force-directed placement. *Softw. Pract. Exp.* **1991**, *21*, 1129–1164. [CrossRef]
209. Hu, Y. Efficient and High Quality Force-Directed Graph Drawing. *Math. J.* **2005**, *10*, 37–71.
210. Blondel, V.D.; Guillaume, J.-L.; Lambiotte, R.; Lefebvre, E. Fast unfolding of communities in large networks. *J. Stat. Mech. Theory Exp.* **2008**, *2008*, P10008. [CrossRef]
211. Larsson, A. AliView: A fast and lightweight alignment viewer and editor for large datasets. *Bioinformatics* **2014**, *30*, 3276–3278. [CrossRef]
212. Ronquist, F.; Teslenko, M.; van der Mark, P.; Ayres, D.L.; Darling, A.; Höhna, S.; Larget, B.; Liu, L.; Suchard, M.A.; Huelsenbeck, J.P. MrBayes 3.2: Efficient Bayesian phylogenetic inference and model choice across a large model space. *Syst. Biol.* **2012**, *61*, 539–542. [CrossRef]
213. Garcia, P.S.; Jauffrit, F.; Grangeasse, C.; Brochier-Armanet, C. GeneSpy, a user-friendly and flexible genomic context visualizer. *Bioinformatics* **2019**, *35*, 329–331. [CrossRef]
214. Chang, D.; Keinan, A. Principal Component Analysis Characterizes Shared Pathogenetics from Genome-Wide Association Studies. *PLOS Comput. Biol.* **2014**, *10*, e1003820. [CrossRef]
215. Lovley, D.R.; Ueki, T.; Zhang, T.; Malvankar, N.S.; Shrestha, P.M.; Flanagan, K.A.; Aklujkar, M.; Butler, J.E.; Giloteaux, L.; Rotaru, A.E.; et al. *Geobacter*: The microbe electric's physiology, ecology, and practical applications. *Adv. Microb. Physiol.* **2011**, *59*, 1–100. [CrossRef] [PubMed]
216. Anderson, R.T.; Vrionis, H.A.; Ortiz-Bernad, I.; Resch, C.T.; Long, P.E.; Dayvault, R.; Karp, K.; Marutzky, S.; Metzler, D.R.; Peacock, A.; et al. Stimulating the in situ activity of *Geobacter* species to remove uranium from the groundwater of a uranium-contaminated aquifer. *Appl. Environ. Microbiol.* **2003**, *69*, 5884–5891. [CrossRef]
217. Coates, J.D.; Phillips, E.J.; Lonergan, D.J.; Jenter, H.; Lovley, D.R. Isolation of Geobacter species from diverse sedimentary environments. *Appl. Environ. Microbiol.* **1996**, *62*, 1531–1536. [CrossRef] [PubMed]
218. Snoeyenbos-West, O.L.; Nevin, K.P.; Anderson, R.T.; Lovley, D.R. Enrichment of *Geobacter* Species in Response to Stimulation of Fe(III) Reduction in Sandy Aquifer Sediments. *Microb. Ecol.* **2000**, *39*, 153–167. [CrossRef]
219. Li, T.; Zhou, Q. The key role of *Geobacter* in regulating emissions and biogeochemical cycling of soil-derived greenhouse gases. *Environ. Pollut.* **2020**, *266*, 115135. [CrossRef] [PubMed]

220. Lemaire, O.N.; Méjean, V.; Iobbi-Nivol, C. The *Shewanella* genus: Ubiquitous organisms sustaining and preserving aquatic ecosystems. *FEMS Microbiol. Rev.* **2020**, *44*, 155–170. [CrossRef]
221. Lightfield, J.; Fram, N.R.; Ely, B. Across bacterial phyla, distantly-related genomes with similar genomic GC content have similar patterns of amino acid usage. *PLoS ONE* **2011**, *6*, e17677. [CrossRef]
222. Bragg, J.G.; Hyder, C.L. Nitrogen versus carbon use in prokaryotic genomes and proteomes. *Proc. Biol. Sci.* **2004**, *271* (Suppl. S5), S374–S377. [CrossRef]
223. Dugdale, R.C. Nutrient limitation in the Sea: Dynamics, Identification and Significance. *Limnol. Oceanogr.* **1967**, *12*, 685–695. [CrossRef]
224. Ely, B. Genomic GC content drifts downward in most bacterial genomes. *PLoS ONE* **2021**, *16*, e0244163. [CrossRef]
225. Kotloski, N.J.; Gralnick, J.A. Flavin electron shuttles dominate extracellular electron transfer by *Shewanella oneidensis*. *mBio* **2013**, *4*, e00553-12. [CrossRef] [PubMed]
226. Zou, L.; Zhu, F.; Long, Z.-E.; Huang, Y. Bacterial extracellular electron transfer: A powerful route to the green biosynthesis of inorganic nanomaterials for multifunctional applications. *J. Nanobiotechnol.* **2021**, *19*, 120. [CrossRef] [PubMed]
227. Liu, D.; Dong, H.; Bishop, M.E.; Zhang, J.; Wang, H.; Xie, S.; Wang, S.; Huang, L.; Eberl, D.D. Microbial reduction of structural iron in interstratified illite-smectite minerals by a sulfate-reducing bacterium. *Geobiology* **2012**, *10*, 150–162. [CrossRef]
228. Simonte, F.; Sturm, G.; Gescher, J.; Sturm-Richter, K. Extracellular Electron Transfer and Biosensors. In *Bioelectrosynthesis*; Harnisch, F., Holtmann, D., Eds.; Springer International Publishing: Cham, Switzerland, 2019; pp. 15–38.
229. Shi, L.; Squier, T.C.; Zachara, J.M.; Fredrickson, J.K. Respiration of metal (hydr)oxides by *Shewanella* and *Geobacter*: A key role for multihaem *c*-type cytochromes. *Mol. Microbiol.* **2007**, *65*, 12–20. [CrossRef] [PubMed]
230. Salgueiro, C.A.; Morgado, L.; Silva, M.A.; Ferreira, M.R.; Fernandes, T.M.; Portela, P.C. From iron to bacterial electroconductive filaments: Exploring cytochrome diversity using *Geobacter* bacteria. *Coord. Chem. Rev.* **2022**, *452*, 214284. [CrossRef]
231. Holmes, D.E.; Zhou, J.; Smith, J.A.; Wang, C.; Liu, X.; Lovley, D.R. Different outer membrane *c*-type cytochromes are involved in direct interspecies electron transfer to *Geobacter* or *Methanosarcina* species. *mLife* **2022**, *1*, 272–286. [CrossRef]
232. Lovley, D.R. Syntrophy Goes Electric: Direct Interspecies Electron Transfer. *Annu. Rev. Microbiol.* **2017**, *71*, 643–664. [CrossRef]
233. Pereira, I.A.C.; Ramos, A.R.; Grein, F.; Marques, M.C.; Da Silva, S.M.; Venceslau, S.S. A Comparative Genomic Analysis of Energy Metabolism in Sulfate Reducing Bacteria and Archaea. *Front. Microbiol.* **2011**, *2*, 69. [CrossRef]
234. Morgado, L.; Fernandes, A.P.; Dantas, J.M.; Silva, M.A.; Salgueiro, C.A. On the road to improve the bioremediation and electricity-harvesting skills of *Geobacter sulfurreducens*: Functional and structural characterization of multihaem cytochromes. *Biochem. Soc. Trans.* **2012**, *40*, 1295–1301. [CrossRef]
235. Levar, C.E.; Chan, C.H.; Mehta-Kolte, M.G.; Bond, D.R. An inner membrane cytochrome required only for reduction of high redox potential extracellular electron acceptors. *mBio* **2014**, *5*, e02034. [CrossRef]
236. Zacharoff, L.; Chan, C.H.; Bond, D.R. Reduction of low potential electron acceptors requires the CbcL inner membrane cytochrome of *Geobacter sulfurreducens*. *Bioelectrochemistry* **2016**, *107*, 7–13. [CrossRef]
237. Aklujkar, M.; Coppi, M.V.; Leang, C.; Kim, B.C.; Chavan, M.A.; Perpetua, L.A.; Giloteaux, L.; Liu, A.; Holmes, D.E. Proteins involved in electron transfer to Fe(III) and Mn(IV) oxides by *Geobacter sulfurreducens* and *Geobacter uraniireducens*. *Microbiology* **2013**, *159*, 515–535. [CrossRef]
238. Peng, L.; Zhang, X.T.; Yin, J.; Xu, S.Y.; Zhang, Y.; Xie, D.T.; Li, Z.L. *Geobacter sulfurreducens* adapts to low electrode potential for extracellular electron transfer. *Electrochim. Acta* **2016**, *191*, 743–749. [CrossRef]
239. Butler, J.E.; Young, N.D.; Lovley, D.R. Evolution of electron transfer out of the cell: Comparative genomics of six *Geobacter* genomes. *BMC Genom.* **2010**, *11*, 40. [CrossRef]
240. Lloyd, J.R.; Leang, C.; Hodges Myerson, A.L.; Coppi, M.V.; Cuifo, S.; Methe, B.; Sandler, S.J.; Lovley, D.R. Biochemical and genetic characterization of PpcA, a periplasmic *c*-type cytochrome in *Geobacter sulfurreducens*. *Biochem. J.* **2003**, *369*, 153–161. [CrossRef]
241. Butler, J.E.; Kaufmann, F.; Coppi, M.V.; Núñez, C.; Lovley, D.R. MacA, a diheme *c*-type cytochrome involved in Fe(III) reduction by *Geobacter sulfurreducens*. *J. Bacteriol.* **2004**, *186*, 4042–4045. [CrossRef]
242. Liu, Y.; Wang, Z.; Liu, J.; Levar, C.; Edwards, M.J.; Babauta, J.T.; Kennedy, D.W.; Shi, Z.; Beyenal, H.; Bond, D.R.; et al. A trans-outer membrane porin-cytochrome protein complex for extracellular electron transfer by *Geobacter sulfurreducens* PCA. *Environ. Microbiol. Rep.* **2014**, *6*, 776–785. [CrossRef]
243. Jiménez Otero, F.; Chan, C.H.; Bond, D.R. Identification of Different Putative Outer Membrane Electron Conduits Necessary for Fe(III) Citrate, Fe(III) Oxide, Mn(IV) Oxide, or Electrode Reduction by *Geobacter sulfurreducens*. *J. Bacteriol.* **2018**, *200*, e00347-18. [CrossRef]
244. Mehta, T.; Coppi, M.V.; Childers, S.E.; Lovley, D.R. Outer Membrane *c*-Type Cytochromes Required for Fe(III) and Mn(IV) Oxide Reduction in *Geobacter sulfurreducens*. *Appl. Environ. Microbiol.* **2005**, *71*, 8634–8641. [CrossRef]
245. Leang, C.; Qian, X.; Mester, T.; Lovley, D.R. Alignment of the *c*-Type Cytochrome OmcS along Pili of *Geobacter sulfurreducens*. *Appl. Environ. Microbiol.* **2010**, *76*, 4080–4084. [CrossRef]
246. Wang, F.; Gu, Y.; O'Brien, J.P.; Yi, S.M.; Yalcin, S.E.; Srikanth, V.; Shen, C.; Vu, D.; Ing, N.L.; Hochbaum, A.I.; et al. Structure of Microbial Nanowires Reveals Stacked Hemes that Transport Electrons over Micrometers. *Cell* **2019**, *177*, 361–369.e10. [CrossRef]
247. Nevin, K.P.; Kim, B.C.; Glaven, R.H.; Johnson, J.P.; Woodard, T.L.; Methé, B.A.; Didonato, R.J.; Covalla, S.F.; Franks, A.E.; Liu, A.; et al. Anode biofilm transcriptomics reveals outer surface components essential for high density current production in *Geobacter sulfurreducens* fuel cells. *PLoS ONE* **2009**, *4*, e5628. [CrossRef]

248. Holmes, D.E.; Chaudhuri, S.K.; Nevin, K.P.; Mehta, T.; Methé, B.A.; Liu, A.; Ward, J.E.; Woodard, T.L.; Webster, J.; Lovley, D.R. Microarray and genetic analysis of electron transfer to electrodes in *Geobacter sulfurreducens*. *Environ. Microbiol.* **2006**, *8*, 1805–1815. [CrossRef]
249. Zacharoff, L.A.; Morrone, D.J.; Bond, D.R. *Geobacter sulfurreducens* Extracellular Multiheme Cytochrome PgcA Facilitates Respiration to Fe(III) Oxides But Not Electrodes. *Front. Microbiol.* **2017**, *8*, 2481. [CrossRef]
250. Afkar, E.; Reguera, G.; Schiffer, M.; Lovley, D.R. A novel *Geobacteraceae*-specific outer membrane protein J (OmpJ) is essential for electron transport to Fe(III) and Mn(IV) oxides in *Geobacter sulfurreducens*. *BMC Microbiol.* **2005**, *5*, 41. [CrossRef]
251. Rollefson, J.B.; Stephen, C.S.; Tien, M.; Bond, D.R. Identification of an extracellular polysaccharide network essential for cytochrome anchoring and biofilm formation in *Geobacter sulfurreducens*. *J. Bacteriol.* **2011**, *193*, 1023–1033. [CrossRef]
252. Huang, L.; Liu, X.; Ye, Y.; Chen, M.; Zhou, S. Evidence for the coexistence of direct and riboflavin-mediated interspecies electron transfer in *Geobacter* co-culture. *Environ. Microbiol.* **2020**, *22*, 243–254. [CrossRef]
253. Myers, C.R.; Myers, J.M. Cloning and sequence of cymA, a gene encoding a tetraheme cytochrome c required for reduction of iron(III), fumarate, and nitrate by *Shewanella putrefaciens* MR-1. *J. Bacteriol.* **1997**, *179*, 1143–1152. [CrossRef]
254. Shi, L.; Rosso, K.M.; Clarke, T.A.; Richardson, D.J.; Zachara, J.M.; Fredrickson, J.K. Molecular Underpinnings of Fe(III) Oxide Reduction by *Shewanella oneidensis* MR-1. *Front. Microbiol.* **2012**, *3*, 50. [CrossRef]
255. Sturm, G.; Richter, K.; Doetsch, A.; Heide, H.; Louro, R.O.; Gescher, J. A dynamic periplasmic electron transfer network enables respiratory flexibility beyond a thermodynamic regulatory regime. *ISME J.* **2015**, *9*, 1802–1811. [CrossRef]
256. Beliaev, A.S.; Saffarini, D.A. *Shewanella putrefaciens* mtrB encodes an outer membrane protein required for Fe(III) and Mn(IV) reduction. *J. Bacteriol.* **1998**, *180*, 6292–6297. [CrossRef]
257. Beliaev, A.S.; Saffarini, D.A.; McLaughlin, J.L.; Hunnicutt, D. MtrC, an outer membrane decahaem c cytochrome required for metal reduction in *Shewanella putrefaciens* MR-1. *Mol. Microbiol.* **2001**, *39*, 722–730. [CrossRef]
258. Ross, D.E.; Ruebush, S.S.; Brantley, S.L.; Hartshorne, R.S.; Clarke, T.A.; Richardson, D.J.; Tien, M. Characterization of protein-protein interactions involved in iron reduction by *Shewanella oneidensis* MR-1. *Appl. Environ. Microbiol.* **2007**, *73*, 5797–5808. [CrossRef]
259. Pirbadian, S.; Barchinger, S.E.; Leung, K.M.; Byun, H.S.; Jangir, Y.; Bouhenni, R.A.; Reed, S.B.; Romine, M.F.; Saffarini, D.A.; Shi, L.; et al. *Shewanella oneidensis* MR-1 nanowires are outer membrane and periplasmic extensions of the extracellular electron transport components. *Proc. Natl. Acad. Sci. USA* **2014**, *111*, 12883–12888. [CrossRef]
260. Marsili, E.; Baron, D.B.; Shikhare, I.D.; Coursolle, D.; Gralnick, J.A.; Bond, D.R. *Shewanella* secretes flavins that mediate extracellular electron transfer. *Proc. Natl. Acad. Sci. USA* **2008**, *105*, 3968–3973. [CrossRef]
261. Edwards, M.J.; White, G.F.; Norman, M.; Tome-Fernandez, A.; Ainsworth, E.; Shi, L.; Fredrickson, J.K.; Zachara, J.M.; Butt, J.N.; Richardson, D.J.; et al. Redox Linked Flavin Sites in Extracellular Decaheme Proteins Involved in Microbe-Mineral Electron Transfer. *Sci. Rep.* **2015**, *5*, 11677. [CrossRef]
262. Min, D.; Cheng, L.; Zhang, F.; Huang, X.-N.; Li, D.-B.; Liu, D.-F.; Lau, T.-C.; Mu, Y.; Yu, H.-Q. Enhancing Extracellular Electron Transfer of *Shewanella oneidensis* MR-1 through Coupling Improved Flavin Synthesis and Metal-Reducing Conduit for Pollutant Degradation. *Environ. Sci. Technol.* **2017**, *51*, 5082–5089. [CrossRef]
263. Li, H.; Xu, D.; Li, Y.; Feng, H.; Liu, Z.; Li, X.; Gu, T.; Yang, K. Extracellular Electron Transfer Is a Bottleneck in the Microbiologically Influenced Corrosion of C1018 Carbon Steel by the Biofilm of Sulfate-Reducing Bacterium *Desulfovibrio vulgaris*. *PLoS ONE* **2015**, *10*, e0136183. [CrossRef]
264. Zhang, P.; Xu, D.; Li, Y.; Yang, K.; Gu, T. Electron mediators accelerate the microbiologically influenced corrosion of 304 stainless steel by the *Desulfovibrio vulgaris* biofilm. *Bioelectrochemistry* **2015**, *101*, 14–21. [CrossRef]
265. Carr, V.R.; Shkoporov, A.; Hill, C.; Mullany, P.; Moyes, D.L. Probing the Mobilome: Discoveries in the Dynamic Microbiome. *Trends Microbiol.* **2021**, *29*, 158–170. [CrossRef]
266. Attrill, E.L.; Łapińska, U.; Westra, E.R.; Harding, S.V.; Pagliara, S. Slow growing bacteria survive bacteriophage in isolation. *ISME Commun.* **2023**, *3*, 95. [CrossRef]
267. Suttle, C.A. Marine viruses--major players in the global ecosystem. *Nat. Rev. Microbiol.* **2007**, *5*, 801–812. [CrossRef] [PubMed]
268. Braga, L.P.P.; Spor, A.; Kot, W.; Breuil, M.-C.; Hansen, L.H.; Setubal, J.C.; Philippot, L. Impact of phages on soil bacterial communities and nitrogen availability under different assembly scenarios. *Microbiome* **2020**, *8*, 52. [CrossRef]
269. Barrangou, R.; Fremaux, C.; Deveau, H.; Richards, M.; Boyaval, P.; Moineau, S.; Romero, D.A.; Horvath, P. CRISPR provides acquired resistance against viruses in prokaryotes. *Science* **2007**, *315*, 1709–1712. [CrossRef] [PubMed]
270. Lopez-Sanchez, M.-J.; Sauvage, E.; Da Cunha, V.; Clermont, D.; Ratsima Hariniaina, E.; Gonzalez-Zorn, B.; Poyart, C.; Rosinski-Chupin, I.; Glaser, P. The highly dynamic CRISPR1 system of *Streptococcus agalactiae* controls the diversity of its mobilome. *Mol. Microbiol.* **2012**, *85*, 1057–1071. [CrossRef]
271. Samson, J.E.; Magadan, A.H.; Moineau, S. The CRISPR-Cas Immune System and Genetic Transfers: Reaching an Equilibrium. *Microbiol. Spectr.* **2015**, *3*, 209–218. [CrossRef] [PubMed]
272. Wang, H.; Zheng, K.; Wang, M.; Ma, K.; Ren, L.; Guo, R.; Ma, L.; Zhang, H.; Liu, Y.; Xiong, Y.; et al. *Shewanella* phage encoding a putative anti-CRISPR-like gene represents a novel potential viral family. *Microbiol. Spectr.* **2024**, *12*, e0336723. [CrossRef]
273. Pawluk, A.; Staals, R.H.; Taylor, C.; Watson, B.N.; Saha, S.; Fineran, P.C.; Maxwell, K.L.; Davidson, A.R. Inactivation of CRISPR-Cas systems by anti-CRISPR proteins in diverse bacterial species. *Nat. Microbiol.* **2016**, *1*, 16085. [CrossRef]

274. Hwang, S.; Maxwell, K.L. Meet the Anti-CRISPRs: Widespread Protein Inhibitors of CRISPR-Cas Systems. *CRISPR J.* **2019**, *2*, 23–30. [CrossRef]
275. Cury, J.; Jové, T.; Touchon, M.; Néron, B.; Rocha, E.P. Identification and analysis of integrons and cassette arrays in bacterial genomes. *Nucleic Acids Res.* **2016**, *44*, 4539–4550. [CrossRef]
276. Hall, R.M. Integrons and gene cassettes: Hotspots of diversity in bacterial genomes. *Ann. N. Y. Acad. Sci.* **2012**, *1267*, 71–78. [CrossRef] [PubMed]
277. Berg, D.E.; Howe, M.M. (Eds.) *Mobile DNA*; American Society for Microbiology Publications: Washington, DC, USA, 1989.
278. Siguier, P.; Gourbeyre, E.; Varani, A.; Ton-Hoang, B.; Chandler, M. Everyman's Guide to Bacterial Insertion Sequences. *Microbiol. Spectr.* **2015**, *3*, MDNA3-0030-2014. [CrossRef]
279. Pradel, N.; Ji, B.; Gimenez, G.; Talla, E.; Lenoble, P.; Garel, M.; Tamburini, C.; Patrick, F.; Lebrun, R.; Bertin, P.; et al. The First Genomic and Proteomic Characterization of a Deep-Sea Sulfate Reducer: Insights into the Piezophilic Lifestyle of *Desulfovibrio piezophilus*. *PLoS ONE* **2013**, *8*, e55130. [CrossRef] [PubMed]
280. Heidelberg, J.F.; Seshadri, R.; Haveman, S.A.; Hemme, C.L.; Paulsen, I.T.; Kolonay, J.F.; Eisen, J.A.; Ward, N.; Methe, B.; Brinkac, L.M.; et al. The genome sequence of the anaerobic, sulfate-reducing bacterium *Desulfovibrio vulgaris* Hildenborough. *Nat. Biotechnol.* **2004**, *22*, 554–559. [CrossRef] [PubMed]
281. Siguier, P.; Gourbeyre, E.; Chandler, M. Bacterial insertion sequences: Their genomic impact and diversity. *FEMS Microbiol. Rev.* **2014**, *38*, 865–891. [CrossRef] [PubMed]
282. Ding, Y.H.; Hixson, K.K.; Aklujkar, M.A.; Lipton, M.S.; Smith, R.D.; Lovley, D.R.; Mester, T. Proteome of *Geobacter sulfurreducens* grown with Fe(III) oxide or Fe(III) citrate as the electron acceptor. *Biochim. Biophys. Acta* **2008**, *1784*, 1935–1941. [CrossRef]
283. Ferreira, M.R.; Salgueiro, C.A. Biomolecular Interaction Studies Between Cytochrome PpcA From *Geobacter sulfurreducens* and the Electron Acceptor Ferric Nitrilotriacetate (Fe-NTA). *Front. Microbiol.* **2018**, *9*, 2741. [CrossRef]
284. Simon, J.; Hederstedt, L. Composition and function of cytochrome c biogenesis System II. *FEBS J.* **2011**, *278*, 4179–4188. [CrossRef]
285. Lee, P.T.; Hsu, A.Y.; Ha, H.T.; Clarke, C.F. A C-methyltransferase involved in both ubiquinone and menaquinone biosynthesis: Isolation and identification of the *Escherichia coli* ubiE gene. *J. Bacteriol.* **1997**, *179*, 1748–1754. [CrossRef]
286. Franza, T.; Gaudu, P. Quinones: More than electron shuttles. *Res. Microbiol.* **2022**, *173*, 103953. [CrossRef]
287. Pokkuluri, P.R.; Londer, Y.Y.; Yang, X.; Duke, N.E.; Erickson, J.; Orshonsky, V.; Johnson, G.; Schiffer, M. Structural characterization of a family of cytochromes c(7) involved in Fe(III) respiration by *Geobacter sulfurreducens*. *Biochim. Biophys. Acta* **2010**, *1797*, 222–232. [CrossRef]
288. Morgado, L.; Bruix, M.; Pessanha, M.; Londer, Y.Y.; Salgueiro, C.A. Thermodynamic characterization of a triheme cytochrome family from *Geobacter sulfurreducens* reveals mechanistic and functional diversity. *Biophys. J.* **2010**, *99*, 293–301. [CrossRef] [PubMed]
289. Hannigan, R.; Dorval, E.; Jones, C. The rare earth element chemistry of estuarine surface sediments in the Chesapeake Bay. *Chem. Geol.* **2010**, *272*, 20–30. [CrossRef]
290. Gilmour, C.C.; Elias, D.A.; Kucken, A.M.; Brown, S.D.; Palumbo, A.V.; Schadt, C.W.; Wall, J.D. Sulfate-reducing bacterium *Desulfovibrio desulfuricans* ND132 as a model for understanding bacterial mercury methylation. *Appl. Environ. Microbiol.* **2011**, *77*, 3938–3951. [CrossRef]
291. Zhao, J.S.; Manno, D.; Beaulieu, C.; Paquet, L.; Hawari, J. *Shewanella sediminis* sp. nov., a novel Na^+-requiring and hexahydro-1,3,5-trinitro-1,3,5-triazine-degrading bacterium from marine sediment. *Int. J. Syst. Evol. Microbiol.* **2005**, *55*, 1511–1520. [CrossRef]
292. Zhao, J.-S.; Manno, D.; Thiboutot, S.; Ampleman, G.; Hawari, J. *Shewanella canadensis* sp. nov. and *Shewanella atlantica* sp. nov., manganese dioxide- and hexahydro-1,3,5-trinitro-1,3,5-triazine-reducing, psychrophilic marine bacteria. *Int. J. Syst. Evol. Microbiol.* **2007**, *57*, 2155–2162. [CrossRef]
293. Ravenhall, M.; Škunca, N.; Lassalle, F.; Dessimoz, C. Inferring horizontal gene transfer. *PLoS Comput. Biol.* **2015**, *11*, e1004095. [CrossRef] [PubMed]
294. Cuecas, A.; Kanoksilapatham, W.; Gonzalez, J.M. Evidence of horizontal gene transfer by transposase gene analyses in *Fervidobacterium* species. *PLoS ONE* **2017**, *12*, e0173961. [CrossRef]
295. Postgate, J.R.; Campbell, L.L. Classification of *Desulfovibrio* species, the nonsporulating sulfate-reducing bacteria. *Bacteriol. Rev.* **1966**, *30*, 732–738. [CrossRef]
296. Schwalb, C.; Chapman, S.K.; Reid, G.A. The tetraheme cytochrome CymA is required for anaerobic respiration with dimethyl sulfoxide and nitrite in *Shewanella oneidensis*. *Biochemistry* **2003**, *42*, 9491–9497. [CrossRef]
297. Murphy, J.N.; Saltikov, C.W. The cymA gene, encoding a tetraheme *c*-type cytochrome, is required for arsenate respiration in *Shewanella* species. *J. Bacteriol.* **2007**, *189*, 2283–2290. [CrossRef] [PubMed]
298. Fu, H.; Jin, M.; Ju, L.; Mao, Y.; Gao, H. Evidence for function overlapping of CymA and the cytochrome 1 complex in the hewanella oneidensis nitrate and nitrite respiration. *Environ. Microbiol.* **2014**, *16*, 3181–3195. [CrossRef] [PubMed]
299. Dulay, H.; Tabares, M.; Kashefi, K.; Reguera, G. Cobalt Resistance via Detoxification and Mineralization in the Iron-Reducing Bacterium *Geobacter sulfurreducens*. *Front. Microbiol.* **2020**, *11*, 600463. [CrossRef] [PubMed]
300. Mollaei, M.; Timmers, P.H.A.; Suarez-Diez, M.; Boeren, S.; van Gelder, A.H.; Stams, A.J.M.; Plugge, C.M. Comparative proteomics of *Geobacter sulfurreducens* PCA(T) in response to acetate, formate and/or hydrogen as electron donor. *Environ. Microbiol.* **2021**, *23*, 299–315. [CrossRef]

301. Cordova, C.D.; Schicklberger, M.F.; Yu, Y.; Spormann, A.M. Partial functional replacement of CymA by SirCD in *Shewanella oneidensis* MR-1. *J. Bacteriol.* **2011**, *193*, 2312–2321. [CrossRef]
302. Gherardini, P.F.; Wass, M.N.; Helmer-Citterich, M.; Sternberg, M.J. Convergent evolution of enzyme active sites is not a rare phenomenon. *J. Mol. Biol.* **2007**, *372*, 817–845. [CrossRef]
303. Zhou, W.; Nakhleh, L. Convergent evolution of modularity in metabolic networks through different community structures. *BMC Evol. Biol.* **2012**, *12*, 181. [CrossRef]
304. Aono, E.; Baba, T.; Ara, T.; Nishi, T.; Nakamichi, T.; Inamoto, E.; Toyonaga, H.; Hasegawa, M.; Takai, Y.; Okumura, Y.; et al. Complete genome sequence and comparative analysis of *Shewanella violacea*, a psychrophilic and piezophilic bacterium from deep sea floor sediments. *Mol. BioSyst.* **2010**, *6*, 1216–1226. [CrossRef]
305. Brettar, I.; Christen, R.; Höfle, M.G. *Shewanella denitrificans* sp. nov., a vigorously denitrifying bacterium isolated from the oxic-anoxic interface of the Gotland Deep in the central Baltic Sea. *Int. J. Syst. Evol. Microbiol.* **2002**, *52*, 2211–2217. [CrossRef]
306. Schmehl, M.; Jahn, A.; Meyer zu Vilsendorf, A.; Hennecke, S.; Masepohl, B.; Schuppler, M.; Marxer, M.; Oelze, J.; Klipp, W. Identification of a new class of nitrogen fixation genes in *Rhodobacter capsulatus*: A putative membrane complex involved in electron transport to nitrogenase. *Mol. Gen. Genet.* **1993**, *241*, 602–615. [CrossRef]
307. Reyes-Prieto, A.; Barquera, B.; Juárez, O. Origin and evolution of the sodium-pumping NADH: Ubiquinone oxidoreductase. *PLoS ONE* **2014**, *9*, e96696. [CrossRef]
308. Biegel, E.; Schmidt, S.; González, J.M.; Müller, V. Biochemistry, evolution and physiological function of the Rnf complex, a novel ion-motive electron transport complex in prokaryotes. *Cell. Mol. Life Sci.* **2011**, *68*, 613–634. [CrossRef] [PubMed]

Disclaimer/Publisher's Note: The statements, opinions and data contained in all publications are solely those of the individual author(s) and contributor(s) and not of MDPI and/or the editor(s). MDPI and/or the editor(s) disclaim responsibility for any injury to people or property resulting from any ideas, methods, instructions or products referred to in the content.